JOURNAL OF PETROLOGY | VOLUME 38 | NUMBER 2 | PAGES 277–297 | 1997

Crustal Origin for Peralkaline Rhyolites from Kenya: Evidence from U-Series Disequilibria and Th-Isotopes

S. BLACK*, R. MACDONALD AND M. R. KELLY

ENVIRONMENTAL SCIENCE DIVISION, IEBS, LANCASTER UNIVERSITY, LANCASTER LA1 4YQ, UK

RECEIVED JUNE 20, 1994 REVISED TYPESCRIPT ACCEPTED OCTOBER 2, 1996

The Olkaria complex is a recent, peralkaline rhyolite field in the Kenya Rift Valley close to the axial region of the Kenya Dome. U–Th disequilibrium was measured by α-spectrometry in whole rocks and mineral separates from seven geographically and compositionally distinct groups (centres) of rhyolites. Forty-three whole-rock samples show variable Th/U ratios (2·8–6·2) and a large range of ($^{238}U/^{232}Th$) ratios (0·5–1·1); 79% of the rhyolites show U excess. Rocks from some centres plot entirely to the left or right of the equiline, whereas some centres straddle it. Internal isochrons give U–Th ages of between $14{\cdot}6^{+2{\cdot}2}_{-2{\cdot}1}$ and $36{\cdot}2^{+2{\cdot}2}_{-2{\cdot}6}$ ka (2σ) respectively for the Gorge Farm centre and $50{\cdot}5^{+7{\cdot}9}_{-7{\cdot}3}$ ka for the Broad Acres centre. These ages, interpreted as phenocryst crystallization ages, are older than eruption ages by $10^3 - 10^4$ yr. The youngest centre displays ($^{226}Ra/^{230}Th$) > 1, indicating that Ra–Th fractionation has taken place <8000 yr bp. There is a positive correlation between ($^{226}Ra/^{230}Th$) and ($^{238}U/^{230}Th$) ratios for rocks of the youngest centre, indicating that the Ra enrichment and the U enrichment probably occurred during the same event. Closed-system fractionation of observed mineral phases cannot alone explain the U-series disequilibria although it may have contributed to other compositional features of the rhyolites. The degree of U enrichment is related to major and trace element variations in the rhyolites as a whole, in that there is a correlation with peralkalinity and thus with incompatible trace element abundances, in particular Nb, Rb and Zr. There is a good correlation between ($^{238}U/^{230}Th$) and pre-eruptive F contents but not pre-eruptive H_2O contents, consistent with previous suggestions that the rhyolites formed by halogen-fluxed melting of the crust. Compositional variations between groups of rhyolites are related to heterogeneity of the crustal source rocks, degree of partial melting(and thus residual mineralogy) and the composition and abundance of metasomatic fluids.

KEY WORDS: *U–Th disequilibrium; crystallization ages; pre-eruptive volatiles; crustal source rocks; metasomatic fluids*

INTRODUCTION

Understanding the timescales of magma formation and differentiation has been among the aims of ^{238}U-series disequilibrium studies for the past 30 years. For example, phenocryst crystallization ages of various volcanic suites have been recorded by Fukuoka (1974), Fukuoka & Kigoshi (1974), Sampson *et al.* (1984), Reagan (1988), Reagan *et al.* (1992), Schaefer *et al.* (1993) and Black (1994). Clear evidence of crystallization ages and their relationships to eruption ages have been reported only rarely, however (Volpe & Hammond, 1991; Volpe, 1992; Reagan *et al.*, 1992; Schaefer *et al.*, 1993; Black, 1994), and these indicate that relatively short crustal residence times (0–30 ka) are likely. These latter studies have concentrated mainly on basaltic–andesitic systems and although many U-series measurements of rhyolites are available (Sampson *et al.*, 1984; Condomines & Sigmarsson, 1993), few data are available for continental rhyolites.

We present measurements of ^{238}U–^{234}U–^{230}Th–^{226}Ra and ^{232}Th in young rhyolites and minerals determined by high-resolution α-spectrometry, to examine the nature and timescales of the processes involved in magmatic evolution at the Olkaria Complex, Kenya. In particular, we use ^{238}U-series disequilibria in mineral phases and rocks both as a tracer and chronometer of magmatic

*Corresponding author. Telephone: (UK) 01524 594209; fax: (UK) 01524 593985; e-mail: s.black@lancaster.ac.uk

processes and to examine the nature of fluid metasomatism inferred in earlier studies (Macdonald *et al.*, 1987).

GEOLOGICAL BACKGROUND

The Greater Olkaria Volcanic Complex (Clarke *et al.*, 1990), or Naivasha complex (Davies & Macdonald, 1987; Macdonald *et al.*, 1987), is a multicentred volcanic field, ~240 km^2 in area, which lies within the inner trough of the Gregory rift valley in south–central Kenya (Fig. 1a). It is located close to the crest of the so-called Kenya Dome, an area of crustal upwarping. Gravity and isostatic studies (Bechtel *et al.*, 1987) indicate that the Dome is associated with only minor uplift (<1 km; Smith, 1994) and is supported by the loading of anomalous mantle within the lithosphere. The crust beneath the Kenya Dome is ~35 km thick (Mechie *et al.*, 1994) and, underneath a 6 km thick rift infill of volcanic and sedimentary rocks, comprises three primary layers whose composition changes with depth from felsic to mafic and in metamorphic grade from greenschist to granulite. The boundaries between the upper and middle, and middle and lower, crust are at ~12 and 23 km, respectively (Mooney & Christensen, 1994). The upper and middle layers have been extensively intruded by dykes and sills. The lower crust is thought (Mooney & Christensen, 1994) to be a mixture of granulite facies metamorphic rocks, mafic intrusions and mafic rocks underplated onto the base of the crust.

At least 80 small volcanic centres have been recognized at Olkaria (Fig. 1b), overwhelmingly of mildly peralkaline rhyolitic (comenditic) composition. Basalt lavas and pyroclastics do, however, occur peripherally to the field and as components of mixed magma rocks within the complex, and it is likely that basaltic magma underlies the whole field. Trachytes and pantellerites were erupted during early stages of Olkaria's history.

Clarke *et al.* (1990) have proposed the multiphase model for the development of the most recent events at Olkaria summarized in Fig. 1c. Growth of a dominantly trachytic lava and pumice pile was terminated by formation of a caldera fracture, which was associated with the eruption of welded pantelleritic deposits. Early post-caldera activity is represented by a series of lava domes and pyroclastic deposits, the so-called Lower Comendite Member of the Olkaria Comendite Formation. The subsequent Ring Dome Formation (the Middle Comendite Member) was mainly a dome-building phase, and includes a series of arcuate domes extruded along the old caldera fracture (Fig. 1b).

There then followed a period of general resurgence, represented by the Upper Comendite Member, which built superincumbent, short, thick flows, particularly well developed at the northern entrance to Hell's Gate (Fig. 1b). Most recent activity has been associated with the north–south Ololbutot fissure just west of Njorowa Gorge.

CRUSTAL RESIDENCE TIMES OF RHYOLITES

Eruption ages of the Olkaria rhyolites are rather poorly constrained. ^{14}C dates from the neighbouring Longonot volcano have been used to bracket the younger Olkaria events (Clarke *et al.*, 1990). The Lower Comendite Member is older than 9150 ± 110 BP, whereas the Middle Member is younger than that date but older than 3280 ± 150 BP. Carbonized wood from a pumice flow associated with the youngest, Ololbutot, flow gave an age of 180 ± 50 BP. ^{14}C ages were determined for Clarke *et al.* (1990) in the NERC Isotope Laboratory at Keyworth, UK, and corrections have been applied for atmospheric changes with time. Earlier reported ^{14}C ages (e.g. Richardson & Richardson, 1972) are of unknown quality and have been ignored for the purpose of this study. Using regional geological and geomorphological relationships, Clarke *et al.* (1990) inferred that the Lower Member is ~20 000 yr old, the Middle ~8000 yr, the Upper ~6000 yr and the Ololbutot member <400 yr. Rhyolitic volcanism at Olkaria seems, therefore, to have been at least semi-continuous for the last 20 kyr. In this study, we have used U-series disequilibria to estimate the crystallization ages of rhyolites from two Olkaria centres.

U and Th decay series disequilibria

Thorough reviews of the principles underlying the ^{238}U-series disequilibria have been provided elsewhere (Allègre, 1968; Capaldi *et al.*, 1976; Condomines *et al.*, 1988; Gill *et al.*, 1992). Briefly, the ^{238}U–^{230}Th method is based on the restoration with time of equilibrium between the progeny ^{230}Th and parent ^{238}U after initial relative U–Th fractionation during magma evolution. The isochron approach applies this to cogenetic minerals which have different initial degrees of fractionation. The isochron is described by the equation (Allègre, 1968)

$$\left(\frac{^{230}\mathrm{Th}}{^{232}\mathrm{Th}}\right)_t = \left(\frac{^{230}\mathrm{Th}}{^{232}\mathrm{Th}}\right)_0 \mathrm{e}^{-\lambda t} + \left(\frac{^{238}\mathrm{U}}{^{232}\mathrm{Th}}\right)_t (1 - \mathrm{e}^{-\lambda t}). \quad (1)$$

^{232}Th is used as a reference radionuclide for normalization purposes and the parentheses in the equation and subsequent text denote activity concentrations. The

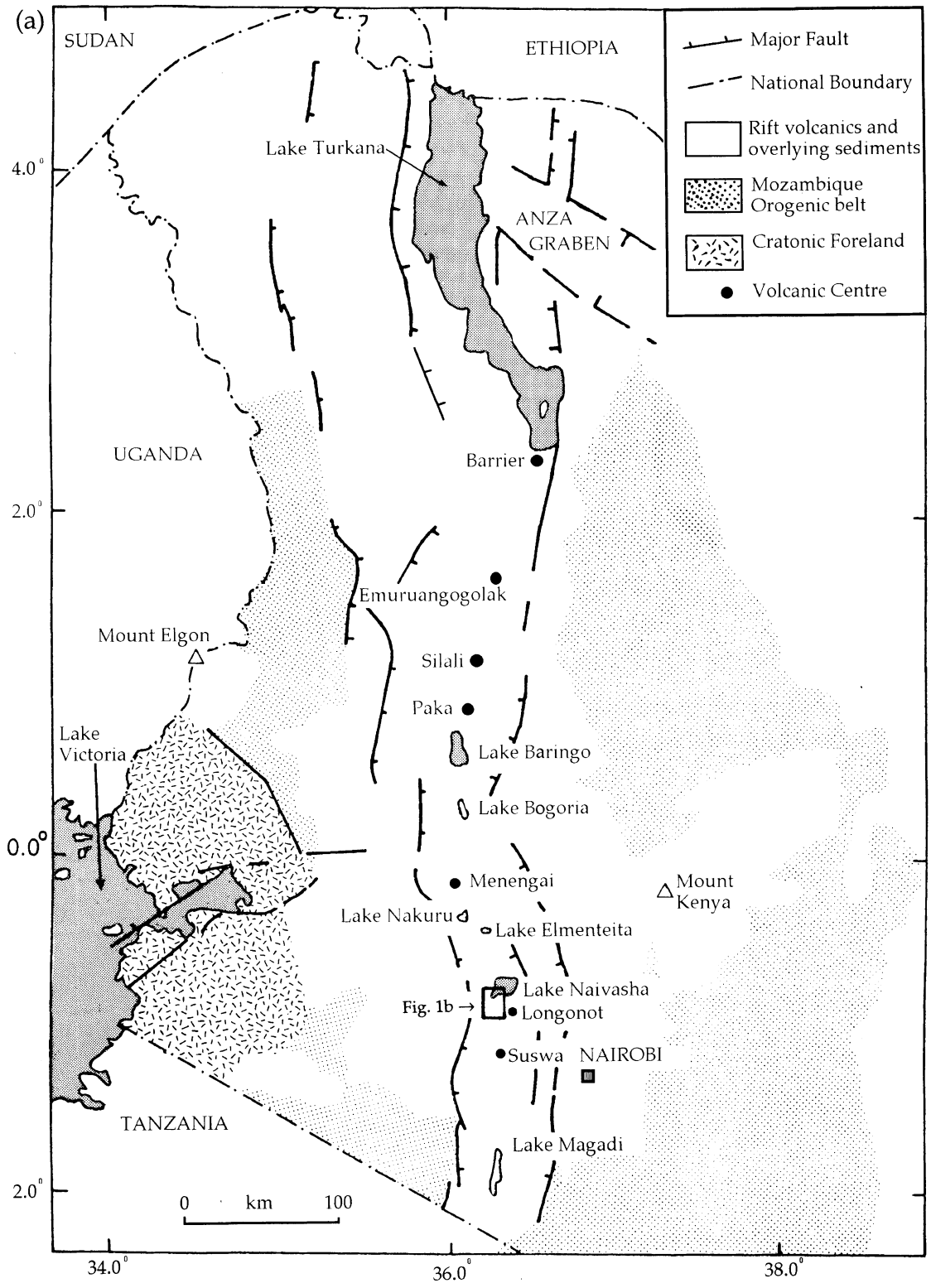

Fig. 1. (a) Map of the Kenya Rift Valley. The Olkaria complex is situated immediately south of Naivasha.

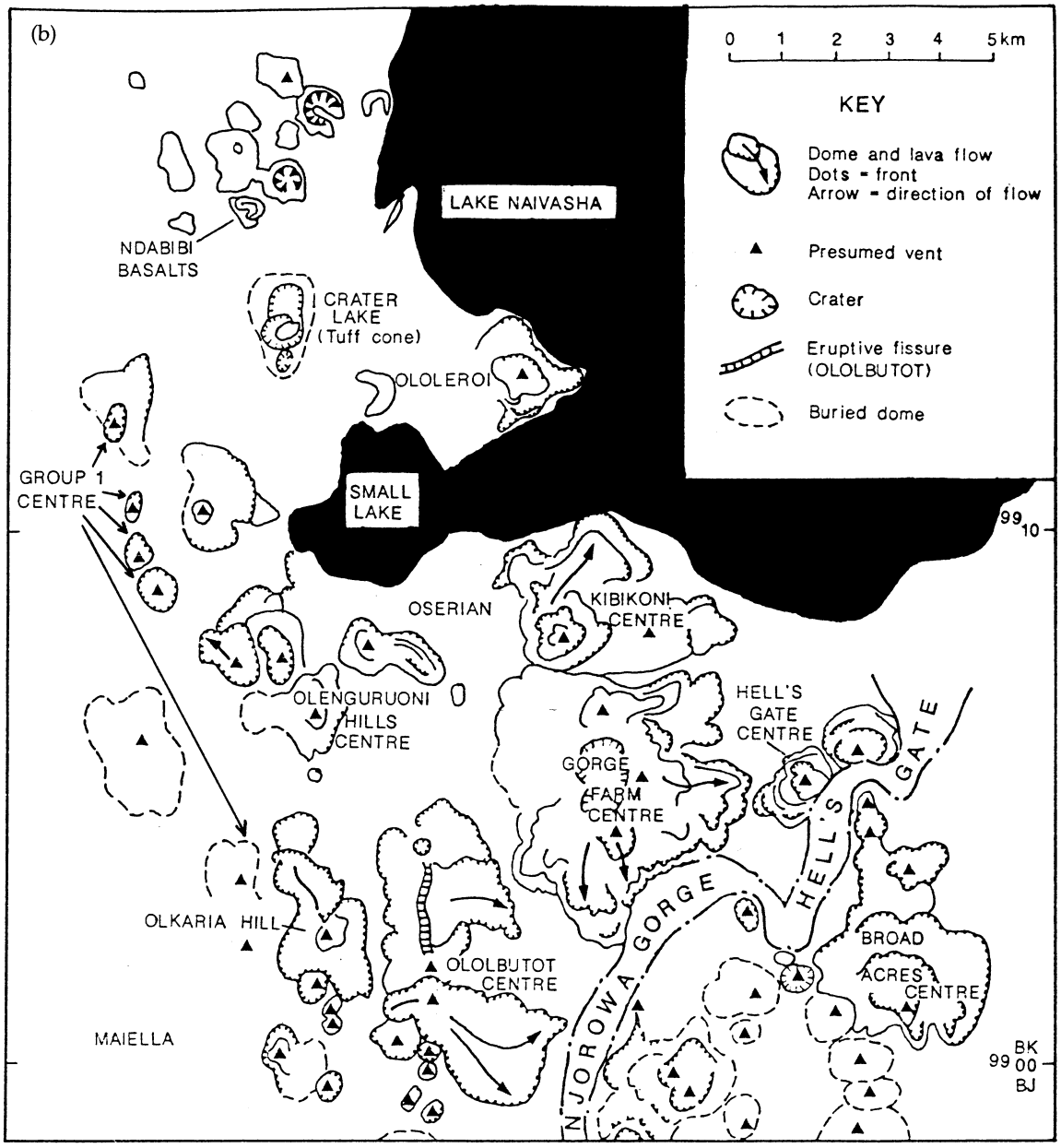

Fig. 1. (b) Map showing the main surface features of the Greater Olkaria Volcanic Complex [modified after Clarke *et al.* (1990)].

half-life of ^{230}Th is taken to be 75·2 kyr, which implies that secular equilibrium would be approached after ~300 kyr.

Analytical procedures and phases separated

Samples studied here come from seven different eruptive centres. Five are from groups of coalesced domes and lava flows forming distinct topographic features (Fig. 1b): Kibikoni and Olenguruoni Hills (Lower Comendite Member), Gorge Farm (Middle Comendite Member) and Broad Acres and Hell's Gate (Upper Comendite Member). A sixth group was erupted from vents aligned along a linear fissure (Ololbutot). Also included here are samples from a string of 10 domes aligned roughly north–south along the western edge of the complex, and thought by Macdonald *et al.* (1987) to be the oldest representatives of the Lower Comendite Member (Group 1). The samples represent much of the geographical and chemical diversity at

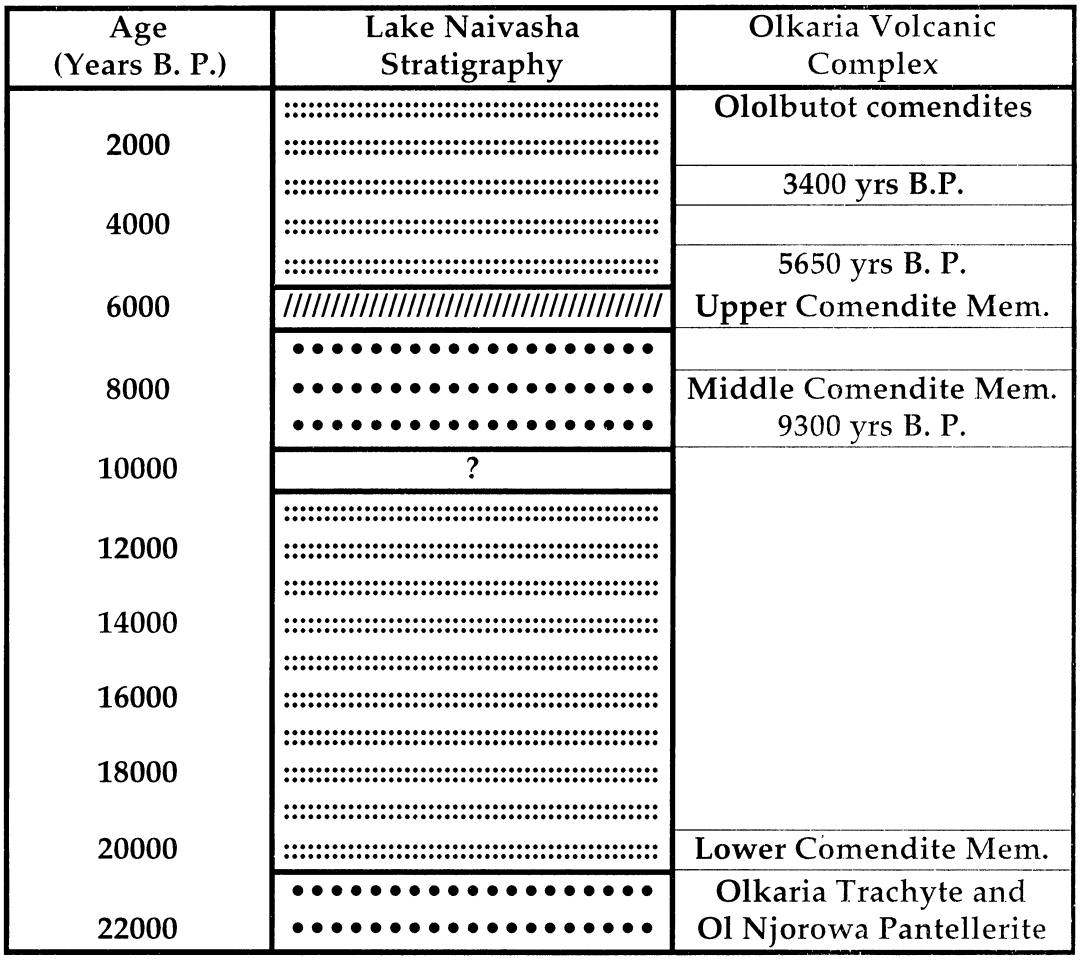

Fig. 1. (c) Stratigraphy of the Olkaria complex. ^{14}C dates and Lake Naivasha high- and low-stands from Clarke *et al.* (1990). ●●, high lake levels; ::::, low lake levels; ///, activity from Longonot volcano.

Olkaria. Samples are listed in the Appendix, which is modified from that of Macdonald *et al.* (1987).

The chemical methods used during this study have been discussed in more detail elsewhere (Black, 1994). Briefly, U-series radionuclides were measured by high-resolution α-spectrometry at Lancaster University. Analysis of whole rocks and mineral separates involved conventional chemical separation techniques (HF–HNO_3–HCl digestion followed by anion exchange separation and electroplating for U and Th).

A ^{232}U–^{228}Th yield monitor was used for U–Th analyses, with a decay and ingrowth correction applied for the daughter ^{224}Ra nuclide. Typical yields ranged from 86 to 100% for uranium, and from 80 to 100% for thorium. Blank and background determinations were carried out frequently on low-background EG&G 'Ultra®' detectors, averaging <10 counts in 10 000 under determinand peaks and <25 counts in 10 000 under the ^{232}U–^{228}Th peaks. Whole-rock and mineral separate masses ranged from 0·5 to 2·0 g and from 0·8 to 5·1 g, respectively, and were generally counted for between 2 and 6 days for whole rocks and between 2 and 10 weeks for mineral separates.

For internal isochrons, phenocryst phases from a single rock sample were used. These were obtained by both magnetic separation and hand picking to an estimated >95% purity for quartz and feldspar. The phenocrysts separated were quartz, alkali feldspar and a magnetic separate containing oxides and other minerals present in the rhyolites, namely, biotite, amphibole, aenigmatite and fayalite. The ages were measured by the slope of the isochrons using a weighted regression method which takes into account the 2σ counting errors associated with each variable (Williamson, 1968).

Table 1: Major and trace element analyses of Olkaria rhyolites

	Olenguruoni Hills				Broad Acres		Gorge Farm		
Sample no:	SB30	302	414	SB29	SB25	SB26	SB27	566	575
wt %									
SiO_2	75·13	75·68	74·15	74·99	74·19	73·98	73·10	73·34	72·64
TiO_2	0·20	0·20	0·21	0·23	0·19	0·19	0·18	0·18	0·18
Al_2O_3	10·90	10·78	10·87	11·36	10·52	10·67	10·33	10·49	10·30
Fe_2O_3*	3·28	3·48	3·38	3·18	3·80	3·87	4·30	4·21	4·44
MnO	0·06	0·08	0·06	0·06	0·06	0·06	0·06	0·06	0·06
MgO	0·06	0·23	0·05	0·08	0·07	0·07	0·05	0·07	0·04
CaO	0·28	0·29	0·31	0·39	0·26	0·18	0·11	0·12	0·10
Na_2O	4·80	5·36	4·88	4·76	4·67	5·50	5·65	5·71	5·68
K_2O	4·53	4·20	4·54	4·64	4·51	4·39	4·34	4·39	4·35
P_2O_5	0·02	0·04	0·01	0·02	0·09	0·02	0·01	0·01	0·01
LOI	0·68	0·52	0·97	0·38	0·83	0·52	0·67	0·73	0·79
Total	99·94	100·86	99·43	100·09	99·19	99·45	98·80	99·31	98·59
p.p.m.									
Ba	301	16	22	50	7	12	1	2	1
Nb	194	188	194	176	355	358	591	525	564
Pb	28	26	26	25	53	52	74	67	71
Rb	245	234	243	233	433	433	692	633	668
Sr	7	5	8	10	6	4	1	3	1
Y	125	121	126	112	202	204	301	269	289
Zn	165	162	171	144	302	292	367	322	357
Zr	933	915	913	849	1620	1626	2304	2041	2198
La	110	116	121	104	143	137	188	129	144
Ce	227	216	240	206	296	286	331	273	306
Nd	89	86	92	79	122	123	139	113	123

Geochemical data for additional specimens from the Olkaria complex (Macdonald *et al.*, 1987). All analyses are by XRF at Edinburgh University.

^{226}Ra was measured using γ-spectrometry of its short-lived daughter ^{214}Pb. Diffusion loss of the intermediate daughter ^{222}Rn from fine-grained material can affect ^{214}Pb activities; to overcome this all samples were sealed in airtight plastic containers. Samples were counted on a low-background Gamma-X high-purity germanium coaxial photon detector, and to keep self-absorption differences negligible, the plastic containers were calibrated for a range of densities and masses.

Major and trace element data for most samples used here have been given by Macdonald *et al.* (1987). Additional analyses are presented in Table 1.

Standards and quality control

There has been extensive discussion of the quality of U–Th data, particularly those generated by α-spectrometry (Capaldi & Pece, 1981; Krishnaswami *et al.*, 1984; Hémond & Condomines, 1985; Gill *et al.*, 1992; McDermott *et al.*, 1993). The accuracy of the Lancaster results can be assessed from our analyses of standards TML and A-THO (Tables 2a and 2b), determined over a 2 yr period. The replicate analyses of the standard (including total dissolutions) show that the mean values are in good agreement with the results of other laboratories. The coefficients of variation (the standard deviation/mean), which express the total random analytical errors, are small, e.g. 1·8% and 1·7% (2σ) for the (^{238}U/^{232}Th) and (^{230}Th/^{232}Th) ratios, respectively, for A-THO and are very close to other reported values (Williams *et al.*, 1992), indicating that analyses by α-spectrometry at Lancaster University are both accurate and reproducible.

Isochron ages

Internal isochrons for samples 570, 575, 565, 566 and SB27 from the Gorge Farm centre are shown in Fig.

Table 2: U-series results (a) for the TML standard and (b) for the A-THO standard

	($^{238}U/^{232}Th$)	($^{230}Th/^{232}Th$)	($^{234}U/^{238}U$)	U (p.p.m.)	Th (p.p.m.)
(a) *For the TML standard*					
LAN L (TIMS)	1·082 ± 0·005	1·084 ± 0·005	1·003 ± 0·005	10·53 ± 2%	29·53 ± 2%
UCSC (α)	1·057 ± 0·038	1·070 ± 0·007	1·004 ± 0·005	10·86 ± 0·033	31·20 ± 0·063
UCSC (TIMS)		1·084 ± 0·004			
OU (TIMS)		1·078 ± 0·020		10·44 ± 0·004	29·46 ± 0·010
Condomines Clermont-Ferrand (TIMS/α)	1·062 ± 0·004	1·081 ± 0·010		10·36 ± 0·060	29·61 ± 0·100
Santa Cruz (TIMS)	1·070 ± 0·003	1·075 ± 0·004	1·004 ± 0·004	10·75 ± 0·030	30·30 ± 0·040
Lancaster (α)	1·040 ± 0·038	1·078 ± 0·026	1·007 ± 0·026	10·78 ± 0·020	29·54 ± 0·080
(b) *For the A-THO standard*					
Condomines Clermont-Ferrand (TIMS/α)	0·907 ± 0·009	1·029 ± 0·014		2·24 ± 0·5%	7·48 ± 0·5%
OU (TIMS)	0·919 ± 0·009	1·018 ± 0·009		2·22 ± 0·001	7·34 ± 0·010
Santa Cruz (TIMS)	0·919 ± 0·002	1·015 ± 0·004	1·007 ± 0·003	2·27 ± 0·003	7·49 ± 0·009
Lancaster (α)	0·912 ± 0·009	1·019 ± 0·009	0·999 ± 0·012	2·27 ± 0·056	7·50 ± 0·150

(a) Results for the TML standard run at Lancaster, compared with other laboratory results, by Williams *et al.* (1992) (mean of eight analyses). Lancaster result is the mean of three analyses. Errors quoted are 2σ. (b) Results for the A–THO standard run at Lancaster compared with results for the same standard, by Williams *et al.* (1992) (mean of three analyses). Lancaster result is the mean of 12 analyses. Errors quoted are 2σ.

2a–e and the data are given in Table 3. Quartz and feldspar have similar Th/U ratios (3·68–4·3 and 3·77–4·31, respectively), with almost identical mean ratios (3·99 ± 0·26 and 4·00 ± 0·28, respectively). Quartz has significantly higher U and Th concentrations (U = 5·8–7·6 p.p.m. and Th = 23·9–28·8 p.p.m.) than feldspar (U = 1·1–4·4 p.p.m. and Th = 4·0–6·2 p.p.m.). α_U and α_{Th} values, the U and Th concentration ratios between the minerals and the corresponding glasses, for the feldspars are similar to other reported values (Condomines *et al.*, 1982; Gill *et al.*, 1992); however, quartz α_U and α_{Th} values are an order of magnitude higher than other reported values (mean $\alpha_U = 0{\cdot}182 \pm 0{\cdot}03$, mean $\alpha_{Th} = 0{\cdot}224 \pm 0{\cdot}013$). This probably indicates that glass inclusions present in the quartz phenocrysts (Wilding *et al.*, 1993) contain significant U and Th concentrations. ($^{238}U/^{230}Th$) ratios vary only slightly within both feldspar and quartz (0·9–1·1). The magnetic separates have uniformly low Th/U ratios (1·8–2·7, mean = 2·18 ± 0·5), but have high mean α_U and α_{Th} values (0·49 ± 0·24 and 0·30 ± 0·06, respectively). The magnetic separates have large Th–U disequilibria, with ($^{238}U/^{230}Th$) ratios ranging from 1·43 ± 0·015 to 2·11 ± 0·060 (mean = 1·75 ± 0·26).

The internal isochrons from the Gorge Farm centre display two different crystallization ages, those defined by samples 570, 575 and SB27 at $14{\cdot}6^{+2{\cdot}2}_{-2{\cdot}1}$, $9{\cdot}8^{+2{\cdot}4}_{-2{\cdot}3}$ and $13{\cdot}0^{+3{\cdot}8}_{-3{\cdot}6}$ ka (2σ), respectively, and the isochrons defined by samples 565 and 566, $31{\cdot}7^{+6{\cdot}5}_{-6{\cdot}1}$ and $36{\cdot}2^{+2{\cdot}6}_{-2{\cdot}6}$ ka (2σ), respectively. This suggests that at least two periods of crystallization have taken place in the centre, one just before eruption (3280–9150 BP), and another much older, 32–36 ka, giving maximum post-crystallization residence times of between 23 ± 3 and 27 ± 3 kyr (2σ). There is no correlation between the U–Th age and any differentiation index (i.e. Zr) in rocks of the Gorge Farm centre. This could imply sequential injection into, and differentiation of batches of magma within, a chamber or chambers as opposed to the evolution of a single differentiating body.

The internal isochron from the Broad Acres centre (515a) is presented in Fig. 2f. Th and U concentrations in the quartz are high (33 and 8 p.p.m., respectively) and somewhat lower in the feldspar (11 and 3 p.p.m.). The magnetic separate has the highest Th/U of all analysed (2·65) and this may be due to larger proportions of fayalite and/or clinopyroxene in this fraction. The internal isochron age from sample 515a ($50{\cdot}5^{+7{\cdot}9}_{-7{\cdot}3}$ ka) is the oldest in our data set, giving the highest maximum post-crystallization residence time of 47 ± 8 kyr (2σ).

One interpretation of the isochron ages is that the relevant melts incorporated older xenocrysts, perhaps within the magma reservoir. There is no evidence that

Table 3: Internal isochron data for the Gorge Farm centre and the Broad Acres centre

Number	Sample	U (p.p.m.)	Th (p.p.m.)	Th/U	($^{238}U/^{232}Th$)	($^{230}Th/^{232}Th$)	($^{238}U/^{230}Th$)	($^{234}U/^{238}U$)
Gorge Farm centre								
570	Whole rock	32·17	109·60	3·41	0·900 ± 0·007	0·780 ± 0·006	1·154 ± 0·009	0·997 ± 0·010
	Glass	41·59	121·77	2·93	1·047 ± 0·022	0·807 ± 0·005	1·298 ± 0·028	1·017 ± 0·020
	Feldspar	1·390	5·960	4·29	0·716 ± 0·017	0·753 ± 0·011	0·951 ± 0·024	1·000 ± 0·017
	Quartz	7·11	28·86	4·06	0·755 ± 0·036	0·760 ± 0·015	0·993 ± 0·041	0·991 ± 0·016
	Magnetic separate i	24·66	43·64	1·77	1·730 ± 0·028	0·870 ± 0·018	1·989 ± 0·029	1·009 ± 0·017
	Magnetic separate ii	25·09	44·96	1·79	1·711 ± 0·059	0·871 ± 0·029	1·964 ± 0·030	0·999 ± 0·010
566	Whole rock	32·10	98·00	3·05	1·004 ± 0·012	0·811 ± 0·007	1·237 ± 0·019	1·006 ± 0·018
	Glass	31·33	125·42	4·00	0·766 ± 0·012	0·735 ± 0·015	1·042 ± 0·012	0·991 ± 0·027
	Feldspar	1·43	6·16	4·31	0·713 ± 0·013	0·721 ± 0·011	0·989 ± 0·017	0·989 ± 0·027
	Quartz	6·52	28·05	4·30	0·700 ± 0·009	0·720 ± 0·009	0·972 ± 0·011	0·999 ± 0·010
	Magnetic separate	28·63	40·23	1·41	1·681 ± 0·031	0·994 ± 0·013	1·691 ± 0·027	0·998 ± 0·010
565	Whole rock	35·17	128·50	3·65	0·839 ± 0·012	0·758 ± 0·013	1·107 ± 0·016	0·999 ± 0·010
	Glass i	45·42	139·94	3·08	0·995 ± 0·007	0·810 ± 0·009	1·228 ± 0·010	0·991 ± 0·016
	Glass ii	45·91	141·32	3·08	0·996 ± 0·009	0·811 ± 0·010	1·228 ± 0·010	0·995 ± 0·010
	Feldspar i	1·10	4·16	3·79	0·809 ± 0·011	0·746 ± 0·012	1·085 ± 0·011	1·009 ± 0·017
	Feldspar ii	1·11	4·20	3·78	0·811 ± 0·010	0·771 ± 0·009	1·052 ± 0·011	0·998 ± 0·011
	Quartz	7·62	28·82	3·78	0·811 ± 0·011	0·760 ± 0·013	1·067 ± 0·014	1·006 ± 0·028
	Magnetic separate	12·44	31·82	2·56	1·199 ± 0·014	0·841 ± 0·016	1·426 ± 0·015	0·992 ± 0·027
575	Whole rock	29·19	99·99	3·43	0·895 ± 0·011	0·771 ± 0·009	1·161 ± 0·011	0·992 ± 0·020
	Glass	39·88	109·86	2·75	1·113 ± 0·015	0·782 ± 0·009	1·423 ± 0·019	0·991 ± 0·029
	Feldspar	1·05	3·95	3·77	0·814 ± 0·016	0·762 ± 0·016	1·068 ± 0·018	1·003 ± 0·021
	Quartz	5·80	23·86	4·13	0·745 ± 0·010	0·759 ± 0·014	0·982 ± 0·015	0·996 ± 0·015
	Magnetic separate	12·75	27·78	2·18	1·407 ± 0·013	0·816 ± 0·009	1·724 ± 0·020	1·000 ± 0·010
SB27	Whole rock	24·51	90·08	3·68	0·834 ± 0·010	0·754 ± 0·014	1·106 ± 0·016	1·008 ± 0·010
	Glass	39·01	108·71	2·79	1·100 ± 0·012	0·770 ± 0·010	1·429 ± 0·012	0·992 ± 0·027
	Feldspar	1·07	4·44	4·15	0·741 ± 0·011	0·735 ± 0·009	1·008 ± 0·015	1·002 ± 0·006
	Quartz	6·69	25·61	3·83	0·801 ± 0·010	0·741 ± 0·014	1·081 ± 0·016	1·008 ± 0·010
	Magnetic separate	11·93	29·94	2·51	1·221 ± 0·011	0·790 ± 0·010	1·546 ± 0·011	0·999 ± 0·006
Broad Acres centre								
515a	Whole rock	18·47	67·67	3·66	0·837 ± 0·012	0·770 ± 0·014	1·087 ± 0·012	0·992 ± 0·020
	Glass	17·12	54·64	3·19	0·960 ± 0·013	0·829 ± 0·019	1·158 ± 0·020	0·991 ± 0·029
	Feldspar	2·71	11·34	4·18	0·733 ± 0·022	0·730 ± 0·017	1·004 ± 0·025	1·003 ± 0·021
	Quartz	7·76	33·23	4·28	0·716 ± 0·012	0·739 ± 0·015	0·969 ± 0·014	0·996 ± 0·015
	Magnetic separate	10·43	27·62	2·65	1·158 ± 0·038	0·895 ± 0·034	1·294 ± 0·036	1·010 ± 0·019

Results for whole-rock and mineral separates for the Gorge Farm and Broad Acres centres. (i) and (ii) indicate replicate analyses. Errors quoted are 2σ.

the phenocrysts are, in fact, xenocrysts. Thus, Macdonald *et al.* (1987) noted the correlation between whole-rock composition and phenocryst assemblage composition. They also noted that zoning in the phenocrysts is restricted. For example, the alkali feldspars show zonation hardly greater than analytical error.

The U-series data, therefore, indicate that the current magmatic system has existed under Olkaria for at least 50 000 yr and that residence times for the rhyolite magmas have been of the order of up to 47 ± 8 kyr. These estimates are consistent with recent Rb–Sr studies (Heumann *et al.*, 1995). Sr contents in the rhyolites are low (down to <1 p.p.m.) and thus Rb/Sr ratios high (100–700). The high Rb/Sr ratios have resulted in rapid changes in $^{87}Sr/^{86}Sr$, potentially allowing resolution of events on timescales as low as 1000 yr. Preliminary Sr

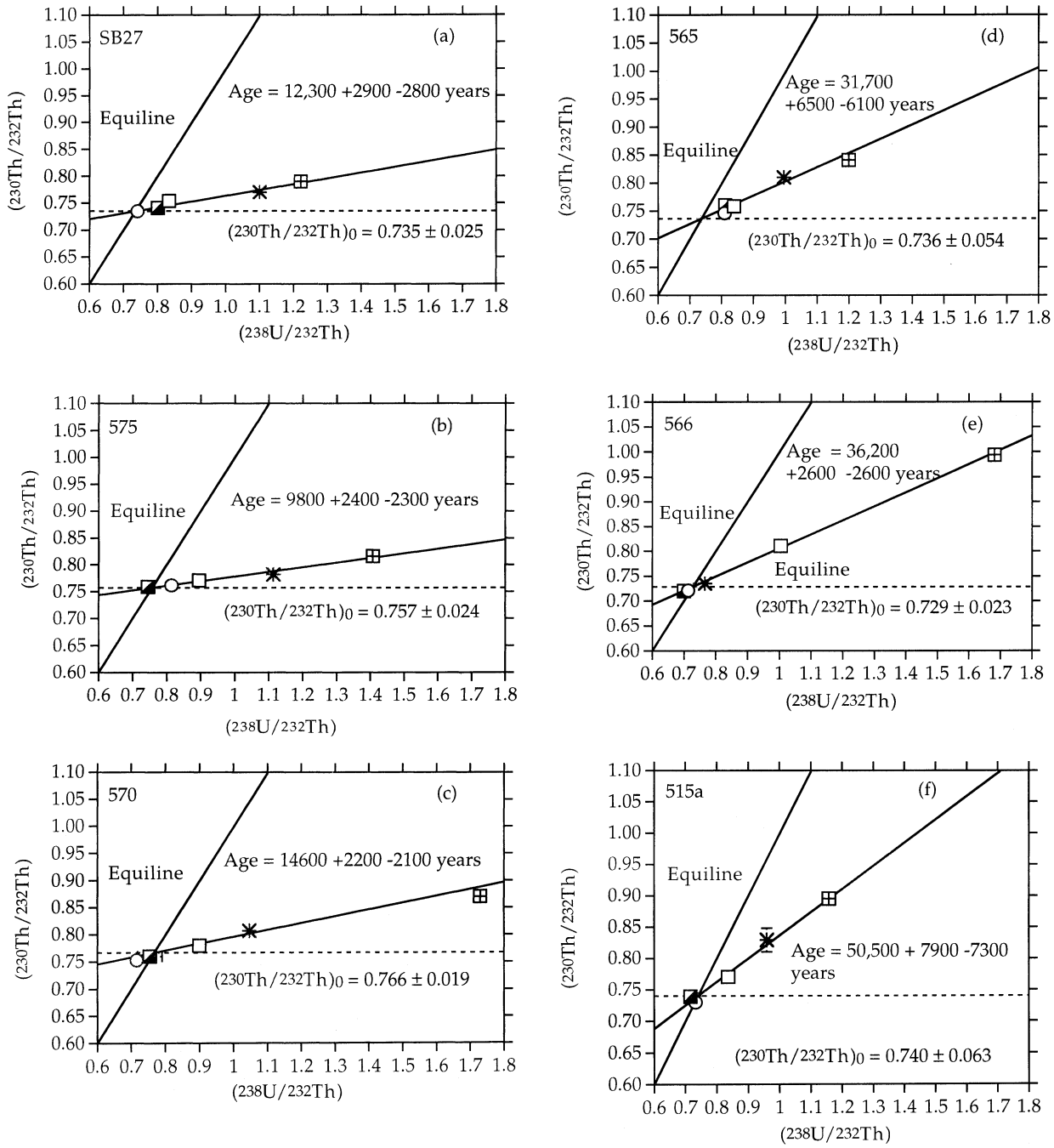

Fig. 2. Internal isochrons for the Olkaria rhyolites. In all plots: open circles, alkali feldspar; diagonally filled square, quartz; open square, whole rock; star, glass; crossed square, magnetic separate. Errors quoted are 2σ.

data on Olkaria rocks erupted at ~9 ka give an isochron age of 70 kyr (Heumann *et al.*, 1995).

Silicic rocks elsewhere have been analysed for U–Th disequilibria, including the climactic eruption of Mt Mazama, dated at 107 ka (Reagan, 1988) and a crystal-rich pumice from the Minoan eruption on Santorini, dated at 100 ka (Pyle, 1990). Together with the earlier studies of Fukuoka (1974) on zircons and the work of Sampson *et al.* (1984), who reported an old (100 ka) age for a recently erupted obsidian dome at Inyo Craters, the

Table 4: ($^{226}Ra/^{230}Th$) ratios for the Olkaria rhyolites

Number	($^{226}Ra/^{230}Th$)
Group 1	
002	1·00 ± 0·04
Olenguruoni	
333	1·01 ± 0·04
Gorge Farm	
570	1·02 ± 0·05
565	0·99 ± 0·07
Hell's Gate	
511d	0·99 ± 0·04
Broad Acres	
515a	0·99 ± 0·05
Ololbutot	
301a	1·15 ± 0·04
346	1·14 ± 0·05
376	1·17 ± 0·04
396	1·11 ± 0·06
399	1·13 ± 0·05

($^{226}Ra/^{230}Th$) ratios for the Olkaria rhyolites. Errors quoted are 2σ.

data demonstrate that rhyolitic magmas may have post-crystallization residence times at shallow levels of the order of 10^4 yr.

The rhyolites from the Ololbutot centre display ($^{226}Ra/^{230}Th$) ratios greater than unity, indicating that they have undergone Ra–Th fractionation in the last 8000 yr (Table 4). The ($^{226}Ra/^{230}Th$) ratios are virtually all identical (from 1·11 ± 0·06 to 1·15 ± 0·04, mean 1·13 ± 0·02) and do not vary with fractionation indices, indicating that the Ra–Th fractionation event is not simply related to magmatic differentiation. Although there is a positive correlation with ($^{238}U/^{230}Th$) ratios, indicating that Ra enrichment and U enrichment may have resulted from the same event, not all the samples have ($^{238}U/^{230}Th$) >1. This may indicate that the range in observed ($^{226}Ra/^{230}Th$) ratios may be caused by a temporal, rather than a chemical process.

GEOCHEMISTRY

The Olkaria rhyolites range from trivially peralkaline {agpaitic index, AI [= mol. $(Na_2O + K_2O)/Al_2O_3$] = 1·02} to almost pantelleritic (AI = 1·40). The major element variations are typical of peralkaline rhyolites, namely, increases in Na_2O, FeO_t and halogens, decreases in SiO_2, Al_2O_3, MgO and CaO, and constant K_2O, with increasing peralkalinity. The rather potassic character of the rocks compared with the majority of comendites led Macdonald *et al.* (1987) to suggest involvement of sialic crust in their genesis.

The rhyolites demonstrate some trace element features characteristic of peralkaline compositions, such as high Nb, Ta, Zn, Zr, Hf and REE, and low Ba, Co, Sc and Sr abundances. The extreme enrichments and depletions of certain elements are notable, however, e.g. Nb (≤1000 p.p.m.), Zr (≤4000 p.p.m.), F (>1%), Sr (≤3 p.p.m.) and Ba (≤5 p.p.m.) (Macdonald *et al.*, 1987; Clarke *et al.*, 1990). Unlike most peralkaline rhyolites, they are also enriched in Cs (≤12·2 p.p.m.), Rb (≤1092 p.p.m.), Th (≤240 p.p.m.) and U (≤43 p.p.m.), resulting, for example, in high Rb/Zr and Th/Ta ratios. Macdonald *et al.* (1987) took this as further evidence for a crustal component in rhyolite genesis.

Sr–Nd–Pb isotopic analyses were carried out on 16 Olkaria rhyolites, including one secondarily hydrated glass, by Davies & Macdonald (1987). The non-hydrated glassy rocks show significant variation in initial $^{87}Sr/^{86}Sr$ (0·7055–0·7116), with relatively little variation in $^{143}Nd/^{144}Nd$ (0·51243–0·51257) and $^{206}Pb/^{204}Pb$ (19·74–19·81). There are no simple correlations between isotopic composition and other geochemical parameters, such as peralkalinity or incompatible trace element (ITE) abundances. The isotopes and trace elements appear to have decoupled during formation or evolution of the rhyolitic magmas.

Although certain compositional features, such as linear correlations between ITE, suggest that the Olkaria rhyolites represent a single liquid-line-of descent, this is too simple an interpretation. Major and trace element and isotopic data indicate that more than one magmatic lineage is involved (Figs 3 and 4). On the basis of such compositional differences, Macdonald *et al.* (1987) recognized seven, stratigraphically restricted, groups of rhyolites. Here we have used a slightly different terminology from that of Macdonald *et al.* (1987). By referring to centres instead of groups, we stress the point that the chemostratigraphic groups tend also to be geographically restricted, e.g. the Gorge Farm and Broad Acres centres (Fig. 1).

Though the number of analyses is rather limited, the isotopic data seem to confirm the presence of several magmatic lineages at Olkaria. Rocks of each centre show relatively little isotope variation, compared with the whole, and are generally distinct from rocks of other centres (Fig. 4). The isotopic distinctions between centres indicate that the melts did not homogenize significantly, providing further evidence for the existence of discrete magma reservoirs.

Th–U ISOTOPIC DATA

The Olkaria rhyolites have unusually high U (≤43 p.p.m.) and Th (≤240 p.p.m.) concentrations (Macdonald *et al.*, 1987; Clarke *et al.*, 1990). Th/U ratios are

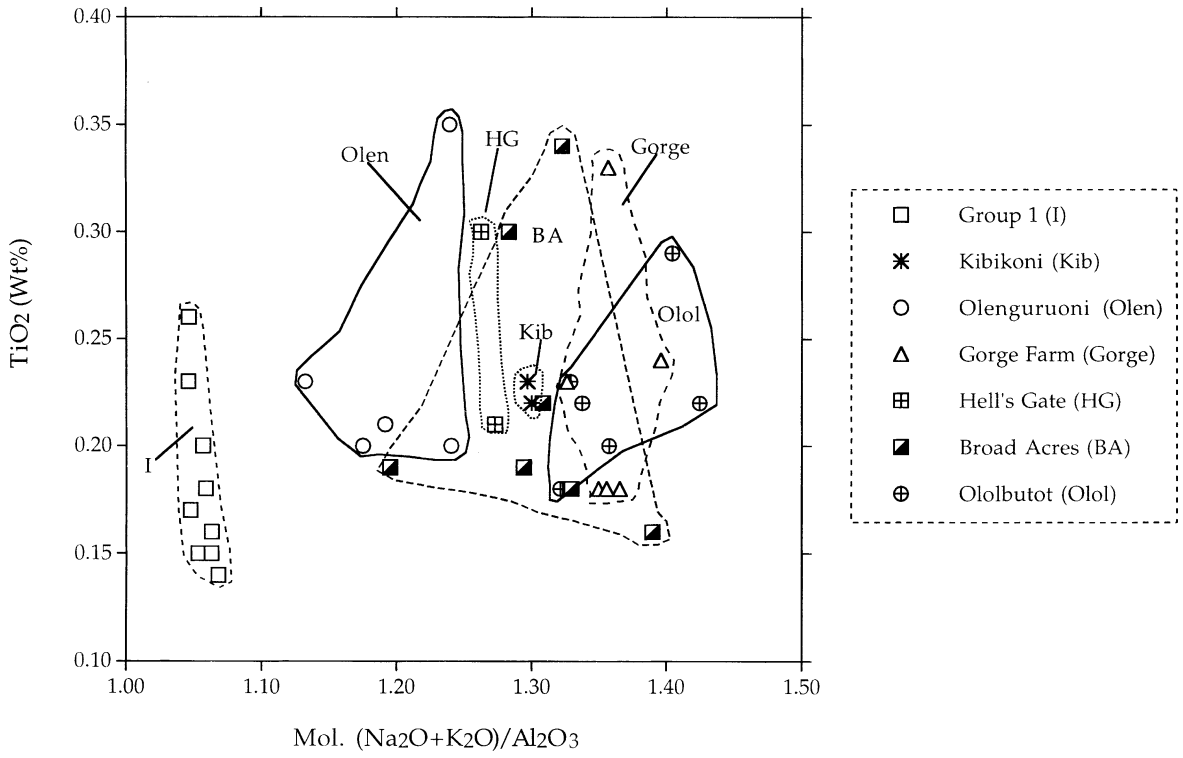

Fig. 3. TiO_2–Agpaitic Index (AI) plot for the Olkaria rhyolites. The rhyolites form a complex multi-lineage relationship. Crystalline and secondarily hydrated samples are omitted, as AI value is affected by loss of Na.

more normal, in that they are fairly close (Fig. 5) to the upper-crustal estimate of 3·8 (Taylor & McLennan, 1985). In detail, however, the most Th and U enriched rocks have lower Th/U ratios.

Whole-rock U-series data are presented in Table 5. A notable feature is the wide spread in ($^{238}U/^{232}Th$), from 30% excess Th to 37% excess U (Fig. 6). Rocks from some centres plot entirely to the left (e.g. Olenguruoni Hills) or right (Gorge Farm) of the equiline, whereas some centres straddle it (Broad Acres and Ololbutot). The majority (79%) show ($^{238}U/^{230}Th$) ratios > 1. U–Th data from subduction zones commonly plot to the right of the equiline and have been interpreted as the result of fluid–source rock interaction occurring before or during partial melting (Gill & Williams, 1990). U is more mobile than Th in the presence of fluids, and it is possible that 'wet' melting of a source produces melts with higher U/Th ratios than the solid residue, the reverse of what happens in 'dry' melting, as in mid-ocean ridge basalts or ocean island basalts where all the melts have ($^{238}U/^{230}Th$) ratios <1 (Gill, 1993). If fluids play a role during partial melting, then the magmas will plot to the right of the equiline. If not, they will be on the left-hand side of the equiline. Thus it seems likely that the majority, but not all, of the Olkaria rhyolites have undergone some form of interaction with fluids during their genesis.

Unlike the Sr–Nd–Pb isotopic ratios, the degree of U enrichment is related to major and trace element variations, in that there is an overall correlation with peralkalinity and thus with the ITE, such as Rb and Zr (Fig. 7a and b), indicating that the enrichment of ^{238}U is intimately related to ITE enrichment and probably resulted from the same process.

PETROGENESIS

In terms of Sr–Nd isotope relationships, it is possible that the Olkaria rhyolites are the extremely fractionated residua of basalts, having undergone feldspar-controlled assimilation–fractional crystallization (AFC). However, Pb isotope systematics clearly demonstrate that the rhyolites and associated basalts are not part of a cogenetic suite (Davies & Macdonald, 1987). The U-series data confirm that the Olkaria basalts and rhyolites are not cogenetic, in that they occupy different fields on the isochron plot (Fig. 8). The rhyolites plot, in fact, close to the composition of average continental crust, which is consistent with major and trace element and isotopic evidence that they were derived from partial melting of crustal rocks (Bailey & Macdonald, 1970; Davies &

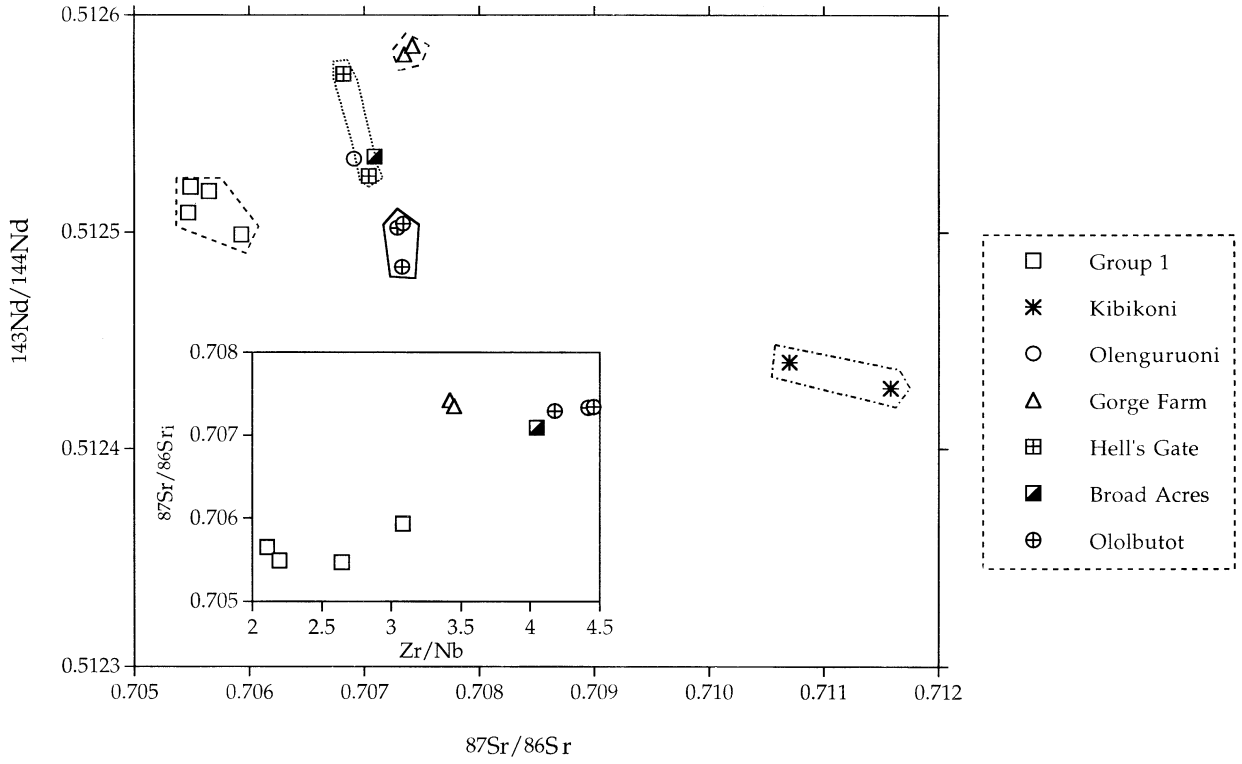

Fig. 4. $^{87}Sr/^{86}Sr$–$^{143}Nd/^{144}Nd$ plot for Olkaria rhyolites. Inset: $^{87}Sr/^{86}Sr$–Zr/Nb plot for the same rocks. The $^{87}Sr/^{86}Sr$–$^{143}Nd/^{144}Nd$ plot indicates that rocks of each centre are isotopically distinct from those of other centres; the $^{87}Sr/^{86}Sr$–Zr/Nb plot indicates that there are at least two different components in the rhyolites.

Macdonald, 1987; Macdonald *et al.*, 1987). Before considering partial melting further, however, we shall use the U-series data to examine the possibility that isotopic variations within the rocks of each centre may have resulted from fractional crystallization. Heumann *et al.* (1995), for example, have suggested that the low (down to <1 p.p.m.) Sr contents in these rocks can only be explained by fractional crystallization involving substantial amounts of feldspar.

We use a simple Rayleigh crystal fractionation model [given by $(1 - F)^{(D_{Th} - D_U)}$], where F is the proportion of melt remaining and D_{Th} and D_U are the mineral separate–glass pairs (Table 3). The crystallizing assemblage (23·8% quartz, 56·4% sanidine, 1·9% clinopyroxene and 0·38% oxides) is that found from linear programming models (Macdonald *et al.*, 1987) to generate satisfactorily the composition of Gorge Farm rocks from Group 1 rocks. The starting (least evolved) composition of the Gorge Farm centre is taken here as sample 570. Removal of the crystallizing assemblage from this starting composition changes Th/U ratios to 0·99 from 1·00, whereas the observed range at the centre is 0·63, i.e. the observed mineral phases cannot sufficiently fractionate Th from U to produce the observed disequilibria range, even within rocks of individual centres.

Further evidence against a simple fractional crystallization model for generation of the rhyolites can be seen from a plot of crystallization age inferred from U–Th vs whole-rock Zr (Fig. 9). If fractional crystallization had been the dominant process for generating the rhyolites then we might have expected to see an increase in Zr content with inferred residence time. This, however, is not the case; the negative trend indicates that there is no simple relationship, at least, between Zr (i.e. ITE) enrichment and potential crystallization time.

U-series disequilibria and the partial melting model

Bailey & Macdonald (1970) and Macdonald *et al.* (1987) established that the Olkaria rhyolites were unusually rich in halogens (F + Cl $\leq$1·5%). Their suggestion, based on various indirect lines of geological and petrological evidence, that the rhyolitic magmas were water poor has not been supported by the results of Wilding *et al.* (1993). By determining water contents of glass (melt) inclusions in quartz phenocrysts, they showed that the pre-eruptive water contents of the magmas were up to 3·4 wt %.

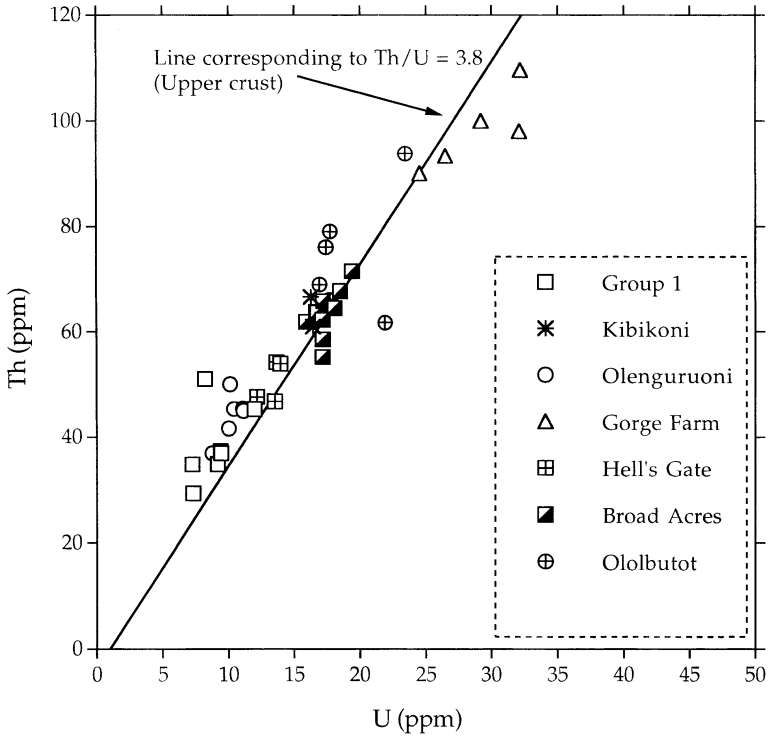

Fig. 5. U vs Th plot for the Olkaria rhyolites.

Total pre-eruptive volatile contents in some magmas must, therefore, have exceeded 4%.

Noting the very high halogen contents of the Olkaria rhyolites, Bailey & Macdonald (1970), Davies & Macdonald (1987) and Macdonald *et al.* (1987) appealed to volatile fluxing as a mechanism for promoting partial melting. The source of the halogens at the site of melting was unknown. One possibility was that intrusion of basaltic magma into the crust raised the local geothermal gradient, setting up a hydrothermal system which scavenged halogens from the surrounding crustal rocks. Alternatively, the halogens may have been derived directly by mantle degassing.

Macdonald *et al.* (1987) tried to relate inter-group differences in ITE abundances to preferential affinity for F or Cl but were unable to demonstrate such an effect; correlation coefficients >0·9 characterize almost all ITE–F or ITE–Cl relationships. They could not preclude a role for hydroxyl complexes, a possibility perhaps strengthened by the recognition that the Olkaria magmas were relatively water rich (Wilding *et al.*, 1993). However, we have not been able to distinguish any significant correlation between pre-eruptive water contents and a trace element or isotopic feature. Macdonald *et al.* (1987) felt that complex formation may help to explain an important feature of LREE behaviour in the Olkaria rocks, namely that they show only moderate correlation with the other incompatible trace elements and have their strongest correlation with peralkalinity, e.g. $r^2 = 0{\cdot}96$ for Ce – molecular $(Na_2O + K_2O)/Al_2O_3$. The LREE may, therefore, have formed complexes of alkali–LREE–silicate type, e.g. $M_3Ce(SiO_4)_2$.

Figures 10 and 11 plot bulk-rock ($^{238}U/^{230}Th$) against F and H_2O abundances, respectively. The volatile data are from the study by Wilding *et al.* (1993) of melt inclusions and are thought to represent pre-eruptive volatile abundances. There is evidence from hydrogen isotopes that some magmas may have partially degassed at depth; the H_2O abundances should, therefore, be viewed as minimum values. Unfortunately, we have no volatile data for the rocks showing the largest U excess, owing to a lack in these rocks of inclusions analysable by ion microprobe. Nevertheless, there is a good correlation, on a small scale of Th/U ratios, between ($^{238}U/^{230}Th$) and F but not between the activity ratio and H_2O. This is consistent with, first, triggering of crustal melting by influx of a halogen-rich fluid, also enriched in U, and, second, fusion of sources which had recently (<0·3 Ma) been metasomatized by such fluids.

There is experimental support for the idea that the existence and nature of such halogen-rich fluids can be examined using U-series disequilibria. Keppler & Wyllie (1990) studied the partitioning of Th and U between granitic melt and aqueous fluids containing variable

Table 5: Whole-rock data for Olkaria rhyolites

Number	($^{238}U/^{232}Th$)	($^{230}Th/^{232}Th$)	($^{238}U/^{230}Th$)	($^{234}U/^{238}U$)	Th (p.p.m.)	U (p.p.m.)	Th/U
Group 1							
002 i	0·774±0·010	0·738±0·010	1·049±0·011	1·010±0·011	37·27±0·29	9·41±0·09	3·96
002 ii	0·775±0·009	0·741±0·009	1·046±0·009	1·004±0·009	37·15±0·31	9·39±0·11	3·96
002 iii	0·778±0·007	0·739±0·006	1·053±0·030	1·004±0·010	37·20±0·32	9·44±0·10	3·94
117c	0·808±0·020	0·717±0·023	1·126±0·031	1·020±0·021	34·84±0·99	9·18±0·17	3·79
143b	0·784±0·010	0·724±0·020	1·083±0·015	1·015±0·020	36·93±0·50	9·44±0·16	3·91
210b	0·815±0·039	0·746±0·023	1·091±0·029	1·028±0·019	45·27±1·55	12·00±0·99	3·76
184a	0·656±0·009	0·637±0·012	1·030±0·020	1·003±0·025	34·78±1·05	7·24±0·65	4·81
372	0·494±0·014	0·642±0·015	0·769±0·016	0·996±0·022	51·00±1·25	8·22±0·67	6·20
105	0·765±0·010	0·811±0·012	0·942±0·019	1·015±0·016	29·35±0·97	7·32±0·26	4·01
Kibikoni Farm centre							
410b i	0·829±0·009	0·711±0·007	1·166±0·008	1·009±0·010	59·50±0·24	16·09±0·11	3·70
410b ii	0·826±0·005	0·714±0·004	1·157±0·007	1·010±0·007	60·94±0·35	16·42±0·13	3·71
583b	0·749±0·004	0·695±0·004	1·077±0·006	1·008±0·006	66·58±0·42	16·26±0·10	4·10
Olenguruoni Hills centre							
414 i	0·621±0·021	0·813±0·019	0·764±0·019	1·010±0·011	49·99±0·87	10·13±0·19	4·93
414 ii	0·622±0·018	0·810±0·016	0·768±0·013	0·995±0·016	49·66±0·97	10·08±0·16	4·93
SB30	0·739±0·013	0·790±0·015	0·936±0·015	1·004±0·020	41·59±0·92	10·03±0·10	4·15
333	0·726±0·024	0·735±0·016	0·988±0·016	0·998±0·022	36·93±0·70	8·75±0·22	4·22
SB29	0·705±0·025	0·745±0·027	0·946±0·025	1·006±0·013	45·29±0·61	10·42±0·13	4·35
302 i	0·760±0·019	0·819±0·016	0·928±0·022	1·009±0·022	44·95±0·38	11·14±0·19	4·04
302 ii	0·750±0·019	0·828±0·018	0·906±0·017	1·012±0·014	45·34±0·39	11·10±0·27	4·09
Gorge Farm centre							
570 i	0·900±0·007	0·780±0·006	1·154±0·009	0·997±0·010	109·60±1·98	32·17±0·59	3·41
570 ii	0·906±0·007	0·782±0·006	1·159±0·008	0·997±0·010	109·90±2·20	32·27±0·69	3·41
504	0·850±0·028	0·780±0·025	1·090±0·018	0·994±0·015	93·37±0·85	26·48±2·30	3·53
566	1·004±0·012	0·811±0·007	1·237±0·019	1·006±0·018	98·00±1·02	32·10±1·51	3·05
565	0·839±0·012	0·758±0·013	1·107±0·016	0·999±0·010	128·50±1·79	35·17±0·42	3·65
575	0·895± 0·011	0·771±0·009	1·161±0·011	0·992±0·020	99·99±1·42	29·19±0·69	3·43
SB27	0·834±0·010	0·754±0·014	1·106±0·016	1·008±0·010	90·08±2·45	24·51±0·54	3·68
Hell's Gate centre							
511d	0·786±0·016	0·771±0·013	1·019±0·025	0·986±0·023	47·57±0·76	12·19±0·27	3·90
551 i	0·803±0·019	0·771±0·019	1·041±0·018	0·994±0·011	54·21±1·11	14·20±0·31	3·82
551 ii	0·808±0·023	0·772±0·018	1·046±0·021	0·995±0·010	53·94±1·09	14·22±0·29	3·79
551 iii	0·802±0·022	0·769±0·022	1·041±0·030	1·010±0·031	54·24±1·18	14·19±0·34	3·82
524/5	0·793±0·022	0·764±0·016	1·039±0·029	1·054±0·035	53·91±1·11	13·95±0·49	3·86
KN19	0·889±0·025	0·801±0·025	1·109±0·033	0·966±0·026	46·73±1·82	13·54±0·49	3·45
Broad Acres centre							
515a i	0·829±0·019	0·769±0·018	1·078±0·022	0·996±0·009	67·47±1·42	18·24±0·18	3·70
515a ii	0·831±0·021	0·771±0·022	1·078±0·022	0·999±0·010	67·91±1·09	18·41±0·22	3·69
515a iii	0·835±0·020	0·779±0·011	1·072±0·019	1·010±0·011	67·55±1·11	18·40±0·21	3·67
515a iv	0·839±0·018	0·772±0·019	1·087±0·018	1·009±0·012	67·25±0·99	18·40±0·28	3·65
515a v	0·837±0·012	0·770±0·014	1·087±0·012	0·992±0·020	67·67±1·52	18·47±0·42	3·66
SB25	0·830±0·015	0·780±0·011	1·065±0·020	1·013±0·022	71·47±0·86	19·38±0·37	3·69
SB26	0·788±0·023	0·782±0·020	1·007±0·030	0·999±0·034	61·83±1·27	15·89±0·45	3·89
512	0·859±0·018	0·753±0·019	1·139±0·026	1·016±0·018	64·48±1·76	18·06±0·35	3·57
605	0·953±0·011	0·801±0·012	1·190±0·015	1·007±0·008	55·19±1·08	17·16±0·18	3·22

Table 5: Whole-rock data for Olkaria rhyolites—continued

Number	($^{238}U/^{232}Th$)	($^{230}Th/^{232}Th$)	($^{238}U/^{230}Th$)	($^{234}U/^{238}U$)	Th (p.p.m.)	U (p.p.m.)	Th/U
KN20 i	0·806±0·009	0·749±0·019	1·076±0·021	1·001±0·005	63·61±1·19	16·72±0·19	3·80
KN20 ii	0·801±0·012	0·747±0·016	1·073±0·019	1·005±0·009	63·67±1·76	16·64±0·21	3·83
KN2	0·841±0·027	0·786±0·023	1·070±0·035	1·032±0·037	62·24±1·86	17·13±0·62	3·63
KN4	0·800±0·014	0·766±0·014	1·045±0·020	0·987±0·019	65·76±1·52	17·18±0·36	3·83
KN21	0·899±0·031	0·788±0·033	1·142±0·043	0·999±0·027	58·49±2·47	17·17±0·49	3·41
Ololbutot centre							
301a i	0·811±0·010	0·773±0·011	1·049±0·011	1·001±0·009	64·01±1·18	16·93±0·25	3·78
301a ii	0·822±0·011	0·780±0·019	1·054±0·020	0·996±0·010	63·69±1·11	17·08±0·21	3·73
301a iii	0·819±0·017	0·774±0·019	1·057±0·025	1·004±0·019	63·57±1·82	16·98±0·37	3·74
399b	0·701±0·011	0·774±0·011	0·906±0·015	1·017±0·028	76·04±1·49	17·39±0·38	4·37
376	1·088±0·013	0·792±0·009	1·373±0·017	1·008±0·014	61·70±1·03	21·91±0·49	2·82
396b	0·667±0·011	0·750±0·012	0·888±0·016	1·020±0·031	79·02±1·54	17·71±0·39	4·46
346	0·782±0·011	0·766±0·011	1·021±0·015	1·017±0·056	93·81±1·79	23·43±0·49	4·00
KN6	0·820±0·018	0·760±0·014	1·078±0·024	0·998±0·025	66·02±1·30	17·65±0·47	3·74
KN9	0·752±0·020	0·752±0·016	1·001±0·027	1·020±0·032	68·92±1·47	16·92±0·54	4·07

Results for the uranium series disequilibrium analyses for 40 whole-rock samples. (i) and (ii) indicate replicate analyses. Errors quoted are 2σ.

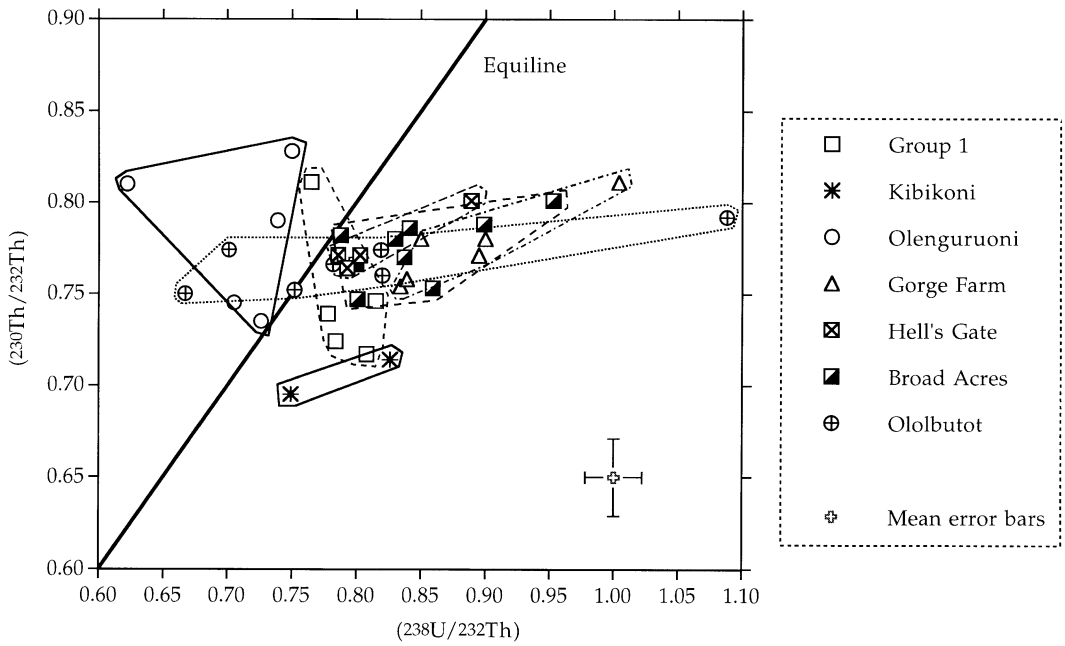

Fig. 6. U–Th isochron diagram for the Olkaria rhyolites. Individual groups are shown, with mean 2σ error bars shown for reference. The multi-lineage nature of the rhyolites is obvious, where rocks of some centres plot entirely to the left of the equiline (e.g. Olenguruoni), or to the right (Gorge Farm), or straddle it (Ololbutot).

amounts of HF, HCl and CO_2, at 2 kbar pressure and 750°C at the oxygen fugacity of the Ni–NiO buffer. They found that the fluid–melt partition coefficients are very low for both Th and U when water is the only volatile present, but that they increase strongly with increasing fluoride concentration, suggesting the formation of fluoride complexes. In contrast, Cl and CO_2 complex with U, but not with Th. Keppler & Wyllie (1990) suggested

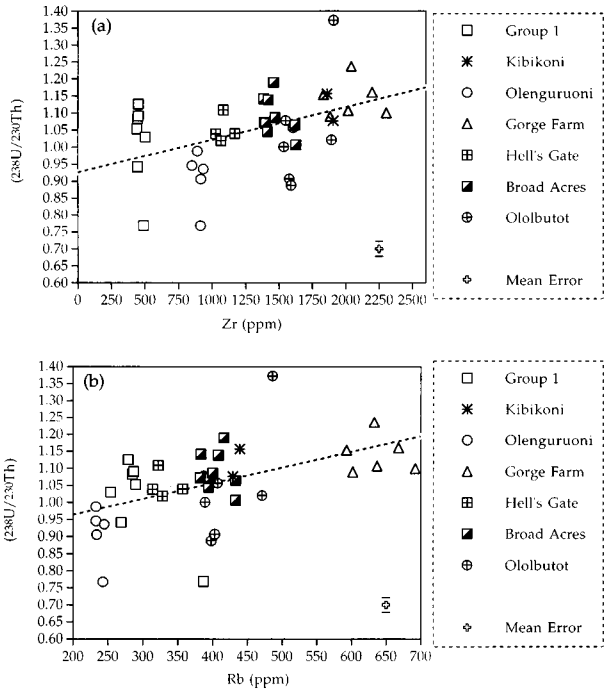

Fig. 7. ($^{238}U/^{230}Th$) vs Zr (a) and Rb (b). The positive relationships, albeit weak, indicate that U enrichment was coupled to ITE enrichment.

that the differing complexing behaviour of Th and U in fluids provides an explanation for the fractionation of Th and U during the formation of volatile-rich magmas, as shown by ^{238}U–^{230}Th disequilibria in young volcanic rocks. Keppler & Wyllie's experiments strictly best represent a melt + fluid + residue scenario and hence will be dependent on the amount of melting. The fluid, however, may also infiltrate the source and cause melting until all of the fluid has been exhausted, producing, therefore, hydrous–halogenated melt + residue. Although Keppler & Wyllie's experiments relate only to the former case, they provide corroboratorive evidence for an incoming F-rich fluid enriched in U.

We conclude that the U-series data are consistent with an origin for the rhyolites by volatile-fluxed partial melting. We now consider more fully the relationship between volatile input and ITE abundances.

Davies & Macdonald (1987) recognized two components in the inferred crustal source rocks. One component has relatively high $^{87}Sr/^{86}Sr$ and Zr/Nb ratios and low $^{143}Nd/^{144}Nd$, and possibly is derived from Pan African (1 Ga) continental crust which underlies this part of central Kenya. The second component has low $^{87}Sr/^{86}Sr$ and Zr/Nb and relatively radiogenic $^{143}Nd/^{144}Nd$, and may have formed by the partial melting of compositionally evolved volcanic rocks of the rift infill sequences (inset Fig. 4). The melting zone may thus span the basement–cover interface, which is ~6 km deep under the Olkaria area (Mechie *et al.*, 1994).

Given that the crustal source rocks were heterogeneous, it is reasonable to suggest that major element (e.g. Ti)

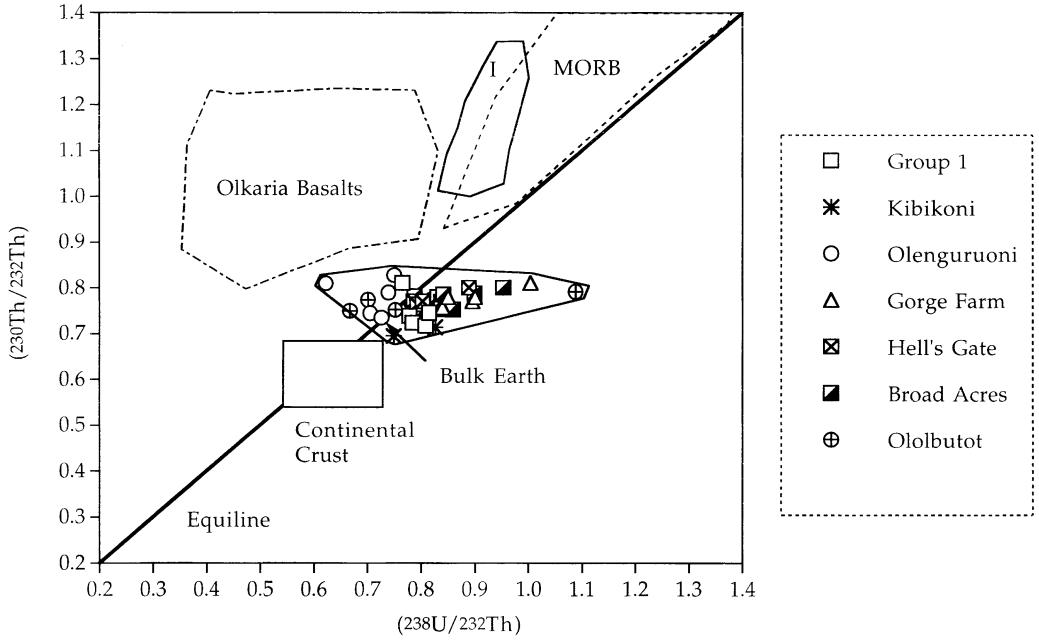

Fig. 8. U–Th isochron diagram for the Olkaria rhyolites, with some comparisons. MORB (mid-ocean ridge basalts), I (Icelandic basalts), Continental Crust and Bulk Earth from Condomines *et al.* (1988) and Gill *et al.* (1992). Olkaria basalts from Black (1994).

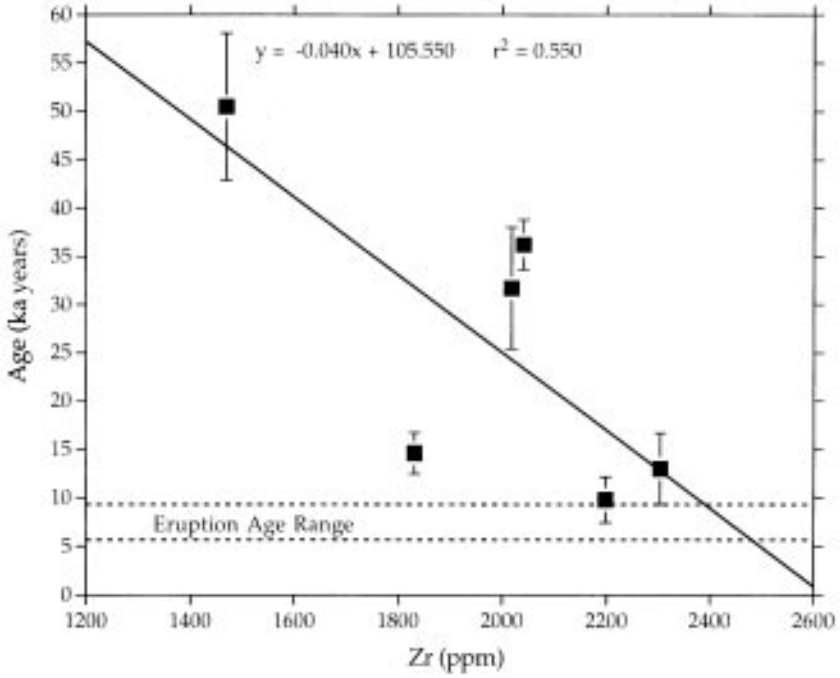

Fig. 9. U–Th age vs whole-rock Zr content for Olkaria rhyolites. The negative trend indicated by the data means that fractional crystallization, which would produce positive trends, is not the only process responsible for the differentiation observed. Eruption age range taken from Clarke *et al.* (1990).

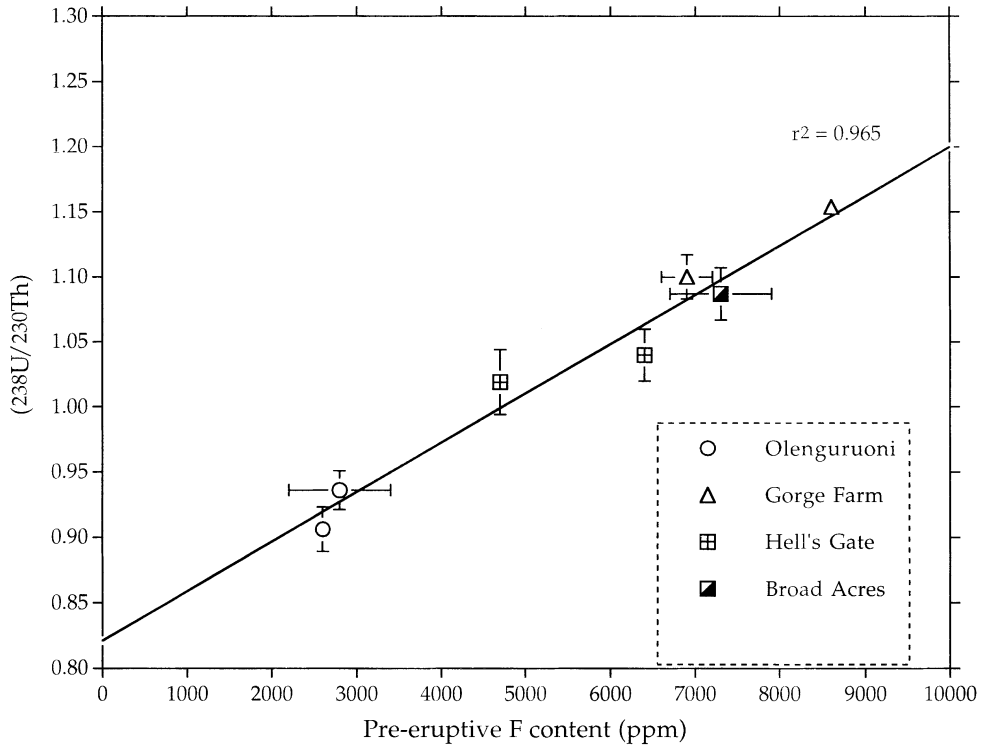

Fig. 10. ($^{238}U/^{230}Th$) vs pre-eruptive F content for Olkaria rhyolites. The ($^{238}U/^{230}Th$) data are whole-rock values from Table 6 and pre-eruptive F values are from inclusions in quartz phenocrysts from the same rocks (Wilding *et al.*, 1993). ($^{238}U/^{230}Th$) errors are 2σ, F errors are derived from multiple analyses of inclusions. Sample numbers used are 414, 333, 511d, 551, 515a, SB27 and 570.

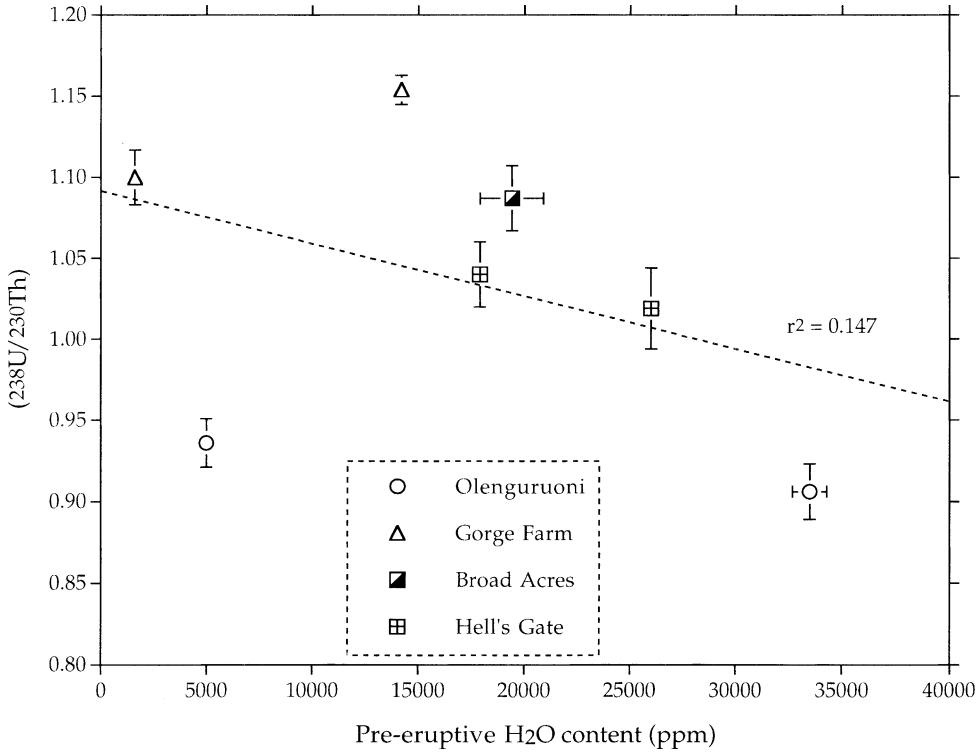

Fig. 11. ($^{238}U/^{230}Th$) vs pre-eruptive H_2O content for Olkaria rhyolites. The ($^{238}U/^{230}Th$) data are whole-rock values from Table 6 and pre-eruptive H_2O values are from inclusions in quartz phenocrysts from the same rocks (Wilding *et al.*, 1993). ($^{238}U/^{230}Th$) errors are 2σ, H_2O errors are derived from multiple analyses of inclusions. Sample numbers are the same as in Fig. 10.

and isotopic differences between groups reflect a combination of different source materials and variable degrees of partial melting. We further suggest that Na contents (and thus the peralkalinity) and the abundances of the HFSE and REE are related to the nature of the incoming volatile phase. Macdonald *et al.* (1987) have already ascribed the peralkaline character of the rhyolites to the formation of melt complexes, possibly including Na-aluminofluoride complexes (Mysen & Virgo, 1985).

Accessory phases such as zircon and monazite strongly influence the HFSE and REE contents of melts when they remain in the residue (Watson, 1979; Harrison & Watson, 1983; Watson & Harrison, 1983; Montel, 1986). Zircon is unstable in peralkaline melts and its stability in a melt decreases with increasing peralkalinity, temperature and water content. At Olkaria, therefore, it is likely that at relatively low levels of F activity and melt peralkalinity, zircon was retained in the restite, causing the low Zr abundances, and thus low Zr/Nb ratios, in the Group 1 rocks. The presence of zircon microphenocrysts in some Group 1 rocks (Macdonald *et al.*, 1987) is consistent with equilibration with restitic zircon. With increasing melt peralkalinity, zircon was melted out of the source rocks, resulting in a sharp increase in Zr/Nb in post-Group 1 rhyolites (Fig. 5). On the basis of zircon solubility studies, Watson (1979) found a 2:1 ratio of excess alkali oxide to ZrO_2 in peralkaline melts and concluded that the Zr forms complexes of the form $Na_4Zr(SiO_4)_2$. Other inferred complexes include Na_2ZrF_6 and Na_3ZrF_7 (Watson, 1979; Collins *et al.*, 1982).

The positive correlation between ($^{238}U/^{230}Th$) and pre-eruptive F indicates that the U enrichment occurred as a result of the input of F-rich fluid to the source region of the rhyolites. Figure 9 also shows that the rhyolites with ($^{238}U/^{230}Th$) ratios <1 have lower pre-eruptive F contents. This implies that there is a critical value of F (0·4–0·5%) at which U enrichment occurs. This does not mean that low F levels encourage Th enrichment, rather that U-bearing zircon remains part of the restite assemblage. Therefore, the rhyolites which have ($^{238}U/^{230}Th$) ratios <1 probably have had zircon in the residue and indeed do have notably lower Zr values (700–900 p.p.m.).

Assuming that accessory phases were no longer residual in the source rocks, the composition of the melts was dependent on three factors:

(1) The amount of volatiles present at the melting site.

(2) The degree of partial melting. Volatile-rich peralkaline melts have low viscosities. Baker & Vaillancourt (1994), for example, have shown that the viscosities of

high-silica peralkaline melts containing 1·5 wt % F and 6 wt % H_2O, i.e. similar to, though higher than, the more volatile-rich Olkaria rhyolites, are of the order of 1×10^3 Pa s at temperatures of ~800°C. Such low viscosities could promote separation from the source rocks of very small-degree melts, enriched in volatiles and ITE.

(3) Davies & Macdonald (1987) showed that some of the compositional variation within the rocks of the different centres may have resulted from AFC processes operating on crustally derived parental magmas. This would have the effect of increasing already high abundances of the ITE.

CONCLUSIONS

(1) ($^{238}U/^{230}Th$) ratios $\neq 1$ in the Olkaria rhyolites indicate that they underwent recent formation (at <350 ka). The rhyolites spread across the equiline on the ($^{230}Th/^{232}Th$)–($^{238}U/^{232}Th$) isochron plot.

(2) An internal isochron gives a U–Th age of $50{\cdot}5^{+7{\cdot}9}_{-7{\cdot}3}$ ka (2σ) for a rock from the Broad Acres centre.

(3) Internal isochrons give U–Th ages of between $14{\cdot}6^{+2{\cdot}2}_{-2{\cdot}1}$ and $36{\cdot}2^{+2{\cdot}6}_{-2{\cdot}6}$ ka (2σ) for rocks from the Gorge Farm centre. The ages are interpreted as phenocryst crystallization ages, are older than eruption ages and of the order of $10^3 - 10^4$ yr, indicating significant post-crystallization residence times. These results are broadly consistent with Sr isotope crystallization ages of the order of 60 ka for Gorge Farm or Broad Acres samples (Heumann *et al.*, 1995).

(4) Rocks of the Ololbutot centre (<400 yr BP) display ($^{226}Ra/^{230}Th$) >1, indicating that Ra–Th fractionation has taken place <8000 yr BP.

(5) Formation of the rhyolites took place between 350 and 50 ka. The small variation in initial ($^{230}Th/^{232}Th$) ratios (from $0{\cdot}729 \pm 0{\cdot}023$ to $0{\cdot}766 \pm 0{\cdot}019$), however, suggests that it is close to the lower figure given the range in ages 9800–50 500 yr. The presence of ($^{226}Ra/^{230}Th$) ratios >1 supports this observation for at least some centres.

(6) Closed-system crystal fractionation of the observed mineral phases cannot explain the magnitude of the U-series disequilibria although it may have contributed to major and trace element variations in each group of rhyolites.

(7) Unlike the Sr–Nd–Pb isotopes, the degree of U enrichment is related to major and trace element variations in the rhyolites as a whole, in that there is an overall correlation with peralkalinity and thus with the ITE, in particular Nb, Rb and Zr.

(8) There is a good correlation between ($^{238}U/^{230}Th$) and pre-eruptive F contents, consistent with previous suggestions that the rhyolites formed by halogen-fluxed melting of the crust.

ACKNOWLEDGEMENTS

We thank Michel Condomines, Chris Hawkesworth, Dave Pyle and Ken Rubin for very helpful reviews of an early version of this manuscript. Lancaster work in Kenya is supported by the Natural Environment Research Council.

REFERENCES

Allègre, C. J., 1968. ^{230}Th dating of volcanic rocks: a comment. *Earth and Planetary Science Letters* **5**, 209–210.

Bailey, D. K. & Macdonald, R., 1970. Petrochemical variations among mildly peralkaline (comenditic) obsidians from the oceans and continents. *Contributions to Mineralogy and Petrology* **28**, 340–345.

Baker, D. R. & Vaillancourt, J., 1994. The viscosity of F + H_2O-bearing peralkaline and peraluminous rhyolitic melts. *Mineralogical Magazine* **58A**, 40–41.

Bechtel, T. D., Forsyth, D. W. & Swain, C. J., 1987. Mechanisms of isostatic compensation in the vicinity of the East African Rift, Kenya. *Geophysical Journal of the Royal Astronomical Society* **90**, 445–465.

Black, S., 1994. U–Th disequilibria systematics of the Olkaria complex, Gregory Rift Valley, Kenya. Unpublished Ph.D. Thesis, University of Lancaster.

Capaldi, G. & Pece, R., 1981. On the reliability of the ^{230}Th–^{238}U dating method applied to young volcanic rocks. *Journal of Volcanology and Geothermal Research* **11**, 367–372.

Capaldi, G., Cortini, M., Gasparini, P. & Pece, R., 1976. Short-lived radioactive disequilibria in freshly erupted volcanic rocks and their implications for the preeruption history of a magma. *Journal of Geophysical Research* **81**, 350–358.

Clarke, M. C. G., Woodhall, D. G., Allen, D. & Darling, G., 1990. Geological, volcanological and hydrogeological controls on the occurrence of geothermal activity in the area surrounding Lake Naivasha, Kenya. Nairobi: Ministry of Energy Report.

Collins, W. J., Beams, S. D., White, A. J. R. & Chappell, B. W., 1982. Nature and origin of A-type granites with particular reference to south-eastern Australia. *Contributions to Mineralogy and Petrology* **80**, 189–200.

Condomines, M., Morand, P., Camus, G. & Duthou, J. L., 1982. Chronological and geochemical study of lavas fron the Chaîne des Puys, Massif Central, France; evidence for crustal contamination. *Contributions to Mineralogy and Petrology* **81**, 296–303.

Condomines, M. & Sigmarsson, O., 1993. Why are so many arc magmas close to ^{238}U–^{230}Th radioactive equilibrium? *Geochimica et Cosmochimica Acta* **57**, 4491–4497.

Condomines, M., Hémond, C. & Allègre, C. J., 1988. U–Th–Ra radioactive disequilibria and magmatic processes. *Earth and Planetary Science Letters* **90**, 243–263.

Davies, G. R. & Macdonald, R., 1987. Crustal influences in the petrogenesis of the Naivasha basalt–comendite complex: combined trace element and Sr–Nd–Pb isotope constraints. *Journal of Petrology* **28**, 1009–1031.

Fukuoka, T., 1974. Ionium dating of acidic volcanic rocks. *Geochemical Journal* **8**, 109–116.

Fukuoka, T. & Kigoshi, K., 1974. Discordant Io-ages and the U, Th distribution between zircon and host. *Geochemical Journal* **8**, 117–122.

Gill, J. B., 1993. Melts and metasomatic fluids: evidence from U-series disequilibria and Th isotopes. *Philosophical Transactions of the Royal Society of London, Series A* **342**, 79–90.

Gill, J. B. & Williams, R. W., 1990. Th isotope and U series studies of subduction-related volcanic rocks. *Geochimica et Cosmochimica Acta* **54**, 1427–1442.

Gill, J. B., Pyle, D. M. & Williams, R. W., 1992. Igneous rocks. In: Ivanovich, M. & Harmon, R. S. (eds) *Uranium Series Disequilibrium Applications to Environmental Problems*. Oxford: Oxford University Press, 909 pp.

Harrison, T. M. & Watson, E. B., 1983. Kinetics of zircon dissolution and zirconium diffusion in granitic melts of variable water content. *Contributions to Mineralogy and Petrology* **84**, 66–72.

Hémond, C. & Condomines, M., 1985. On the reliability of the ^{230}Th–^{238}U dating method applied to young volcanic rocks—discussion. *Journal of Volcanology and Geothermal Research* **26**, 365–368.

Heumann, A., Davies, G. R., Elliot, T. R., Staudigel, H., Freedman, P. & Kara, A., 1995. Magma chamber residence times: a Sr–Th isotope study of high silica rhyolites in Kenya. *European Geophysical Union Abstracts XI*-**4**, 135.

Keppler, H. & Wyllie, P. J., 1990. Role of fluids in transport and fractionation of uranium and thorium in magmatic processes. *Nature* **348**, 531–533.

Krishnaswami, H. C. S., Turekian, K. K. & Bennett, J. T., 1984. The behaviour of the ^{232}Th and the ^{238}U decay chain nuclides during magma formation and volcanism. *Geochimica et Cosmochimica Acta* **48**, 505–511.

Macdonald, R., Davies, G. R., Bliss, C. M., Leat, P. T., Bailey, D. K. & Smith, R. L., 1987. Geochemistry of high-silica peralkaline rhyolites, Naivasha, Kenya Rift Valley. *Journal of Petrology* **28**, 979–1008.

McDermott, F., Elliot, T. R., van Calsteren, P. & Hawkesworth, C. J., 1993. Measurement of ^{230}Th/^{232}Th ratios in young volcanic rocks by single-sector thermal ionising mass spectrometry. *Chemical Geology* **103**, 283–292.

Mechie, J., Keller, G. R., Prodehl, C., Gaciri, S., Braile, L. W., Mooney, W. D., Gajewski, D. & Sandmeier, K.-J., 1994. Crustal structure beneath the Kenya Rift from axial profile data. *Tectonophysics* **236**, 179–200.

Montel, J. M., 1986. Experimental determination of the solubility of Ce-monazite in SiO_2–Al_2O_3–K_2O–Na_2O melts at 800°C, 2 kbar, under H_2O-saturated conditions. *Geology* **14**, 659–662.

Mooney, W. D. & Christensen, N. I., 1994. Composition of the crust beneath the Kenya rift. *Tectonophysics* **236**, 391–408.

Mysen, B. O. & Virgo, D., 1985. Trace element partitioning and melt structure: an experimental study at 1 atm pressure. *Geochimica et Cosmochimica Acta* **44**, 1917–1930.

Pyle, D. M., 1990. Geological and radiochemical studies on young volcanoes: Santorini, Greece and Oldoinyo Lengai, Tanzania. Unpublished Ph.D. Thesis, University of Cambridge.

Reagan, M. K., 1988. U series equilibrium and disequilibrium in plagioclase from Arenal Volcano, Costa Rica. *Transactions of the American Geophysical Union (EOS)* **69**, 1509.

Reagan, M. K., Volpe, A. M. & Cashman, K. V., 1992. ^{238}U- and ^{232}Th-series chronology of phonolite fractionation at Mount Erebus, Antarctica. *Geochimica et Cosmochimica Acta* **56**, 1401–1407.

Richardson, J. L. & Richardson, A. E., 1972. History of an African rift lake and its climatic implications. *Ecological Monograph* **42**, 499–534.

Sampson, D. E., Williams, R. W., Robin, M. & Gill, J. B., 1984. The age of rhyolitic magma at eruption, Inyo volcanic chain, eastern California. *Transactions of the American Geophysical Union (EOS)* **65**, 1129.

Schaefer, S. J., Sturchio, N. C., Murrell, M. T. & Williams, S. N., 1993. Internal ^{238}U-series systematics of pumice from the November 13, 1985, eruption of Nevado del Ruiz, Colombia. *Geochimica et Cosmochimica Acta* **57**, 1215–1219.

Smith, M., 1994. Stratigraphic and structural constraints on mechanisms of active rifting in the Gregory Rift, Kenya. *Tectonophysics* **236**, 3–22.

Taylor, S. R. & McLennan, S. M., 1985. *The Continental Crust; its Composition and Evolution*. Oxford: Blackwell, 312 pp.

Volpe, A. M., 1992. ^{238}U–^{230}Th–^{226}Ra disequilibrium in young Mt. Shasta andesites and dacites. *Journal of Volcanology and Geothermal Research* **53**, 227–238..

Volpe, A. M. & Hammond, P. E., 1991. ^{238}U–^{230}Th–^{220}Ra disequilibrium in young Mount St. Helens volcanics: time constraints for magma formation and crystallization. *Earth and Planetary Science Letters* **107**, 475–486.

Watson, E. B., 1979. Zircon saturation in felsic liquids: experimental results and applications to trace element geochemistry. *Contributions to Mineralogy and Petrology* **70**, 407–419.

Watson, E. B. & Harrison, T. M., 1983. Zircon saturation revisited: temperature and composition effects in a variety of crustal magma types. *Earth and Planetary Science Letters* **64**, 295–304.

Wilding, M. C., Macdonald, R., Davies, E. & Fallick, A. E., 1993. Volatile characteristics of peralkaline rhyolites from Kenya: an ion microprobe, infrared spectroscopic and hydrogen isotope study. *Contributions to Mineralogy and Petrology* **114**, 264–275.

Williams, R. W., Collerson, K. D., Gill, J. B. & Deniel, C., 1992. High Th/U ratios in subcontinental lithospheric mantle: mass spectrometric measurements of Th isotopes in Gaussberg lamproites. *Earth and Planetary Science Letters* **111**, 257–268.

Williamson, J. H., 1968. Least-squares fitting of a straight line. *Journal of Physics* **46**, 1845–1847.

APPENDIX 1: SAMPLE LOCALITIES, DESCRIPTION AND PHENOCRYST ASSEMBLAGES

Sample no.	Coordinates	Description	Phenocrysts
Group 1			
002	AK 942 100	Obsidian flow	F+Ox+Z
117	AK 943 165	Pumiceous obsidian flow	Aphyric
143b	AK 958 107	Obsidian flow	Aphyric
210b	AK 946 120	Fissured obsidian flow	Aphyric
184a	Ak 924 104	Pumiceous crystalline dome	F+Ox+Z
372	AK 959 026	Pumiceous crystalline flow	Q+F+QF+Ox
Kibikoni Farm			
410b	AK 998 085	Obsidian flow	Aphyric
583b	BK 035 080	Obsidian flow	Aphyric
Olenguruoni			
414	AK 946 085	Pumiceous obsidian flow	Q+F+Ox
SB30	AK 946 080	Obsidian flow	Q+F+Ox
333	AK 942 072	Obsidian flow	Q+F+Ox
SB29	AK 946 077	Obsidian flow	Q+F+Ox
302	AK 935 079	Obsidian flow	Q+F+Ox
Gorge Farm			
570	BK 035 061	Obsidian flow NE	Q+F+Ox+Fa+Ab+Ae
504	BK 036 039	Obsidian flow S	Q+F+QF+Ox+Fa+Ab+Bi
566	BK 042 049	Obsidian flow E	Q+F+Fa+Ab+Bi+Ox
565	BK 030 053	Obsidian flow E	Q+F+Fa+Ab+Bi+Ox
575	BK 023 063	Obsidian flow NNE	Q+F+Fa+Ab+Ae+Ox
SB27	BK 035 044	Obsidian flow S	Q+F+Fa+Ab+Bi+Ox
Hell's Gate			
511d	BK 062 054	Obsidian flow	Q+F+Px
551	BK 062 035	Obsidian flow	Q+F+Px
524/5	BK 069 039	Pumice clasts in air-fall tuff	Aphyric
KN19	BK 076 043	Obsidian flow	Q+F
Broad Acres			
515a	BK 042 029	Obsidian flow	Q+F+Fa+Ox
SB25	BK 065 048	Crystalline comendite interior	Aphyric
SB26	BK 065 048	Obsidian flow base to SB25	Aphyric
512	BK 064 051	Obsidian chill of plug	Aphyric
605	BK 064 049	Obsidian flow	Aphyric
KN20	BK 081 025	Obsidian flow	F
KN2	BK 049 018	Obsidian flow	Aphyric
KN4	BK 053 018	Obsidian flow	Aphyric
KN21	BK 079 017	Obsidian flow	Aphyric
Ololbutot			
301a	BK 007 006	Obsidian flow	Aphyric
399b	AK 971 042	Obsidian flow	Aphyric
376	AK 955 046	Obsidian flow	Aphyric
396b	AK 981 047	Obsidian flow	Aphyric
346	AK 990 033	Obsidian flow	Aphyric
KN6	AK 977 025	Obsidian flow	Aphyric
KN9	AK 980 039	Obsidian flow	Aphyric

Ab, amphibole; Ae, aenigmatite; Bi, biotite; F, feldspar; Fa, fayolite; Ox, oxides; Px, pyroxene; Q, quartz; QF, quartz–feldspar intergrowths; Z, zircon.